Four Different Emissions from a Pt(Bodipy)(PEt$_3$)$_2$(S-Pyrene) Dyad

Peter Irmler,[†] Franciska S. Gogesch,[†] Christopher B. Larsen,[‡] Olvier S. Wenger,[‡] Rainer F. Winter*,[†]

[†]Fachbereich Chemie, Universität Konstanz, Universitätsstraße 10, D-78457 Konstanz, Germany

[‡]Department of Chemistry, University of Basel, St.-Johanns-Ring 19, CH-4056 Basel, Switzerland

ABSTRACT: The Pt(bodipy)–(mercaptopyrene) dyad **BPtSPyr** shows four different emissions: Intense near-infrared phosphorescence (Φ_{ph} up to 15%) from a charge-transfer state pyrS$^{\bullet+}$–Pt–BDP$^{\bullet-}$, additional fluorescence and phosphorescence emissions from the $^1\pi\pi^*$ and $^3\pi\pi^*$ states of the bodipy ligand at r.t., and phosphorescence from the pyrene $^3\pi\pi^*$ and the bodipy $^3\pi\pi^*$ states in a glassy matrix at 77 K.

Content

Experimental Procedures

Methods. Oxidative addition reactions and ligand manipulations were performed under a N_2 atmosphere using standard Schlenk techniques or inside a glove box. C_6D_6, CD_2Cl_2, $CDCl_3$ and THF-*d8* were supplied from Eurisotop. All other solvents were used as received. Complex *trans*-Pt(bodipy)I$(PEt_3)_2$ (**BPtI**) was synthesized according to the literature protocol.[1]

NMR experiments were carried out on a Varian Unity Inova 400, a Bruker Avance III DRX 400 or a Bruker Avance DRX 600 spectrometer. ^{1}H and ^{13}C spectra were referenced to the solvent signal, while ^{31}P and ^{195}Pt spectra were referenced to external standards (85% H_3PO_4 or saturated $K_2[PtCl_6]$ in D_2O, respectively). NMR data are given as follows: chemical shift (δ in ppm), multiplicity (br, broad; d, doublet; dd, doublet of doublets; m, multiplet; s, singlet; t, triplet, vt virtual triplet), integration, coupling constant (Hz). Unequivocal signal assignments were achieved by 2D NMR experiments. The numbering of the nuclei follows that of the chemical structures displayed at the synthesis protocol.

Combustion analysis was conducted with an Elementar vario MICRO cube CHN-analyzer from Heraeus. Luminescence spectra and lifetimes as well as quantum yields were measured in acetone, CH_2Cl_2, 2-MeTHF, THF, or toluene solutions of the complex on a PicoQuant FluoTime 300 spectrometer. Unless stated otherwise, absolute quantum yields were determined with an integrating sphere within the FluoTime 300 spectrometer. Emission spectroscopy under inert gas atmosphere was conducted in a quartz cuvette modified with an angle valve from Normag. The emission data of **BPtSPyr** in acetone with excitation at 405 nm is not reported due to sample decomposition upon laser excitation.

UV/Vis/NIR spectra were recorded on a TIDAS fiber optic diode array spectrometer (combined MCS UV/NIR and PGS NIR instrumentation) from J&M in HELLMA quartz cuvettes with 0.1 cm optical path lengths.

Transient absorption spectroscopy was performed using an LP920-KS instrument from Edinburgh Instruments. 410 nm and 470 nm excitation were obtained from pulsed third-harmonic radiation from a Quantel Brilliant b Nd:YAG laser equipped with a Rainbow optical parameter oscillator (OPO). 532 nm excitation was obtained from pulsed second-harmonic generation from a Quantel Brilliant b Nd:YAG laser. The laser pulse duration was ~10 ns and the pulse frequency 10 Hz with a typical pulse energy of 7 mJ. Detection of transient absorption spectra occurred on an iCCD camera from Andor. Single-wavelength kinetics were recorded using a photomultiplier tube. All optical spectroscopic experiments were performed under deaerated conditions using quartz cuvettes in which oxygen can be removed by the freeze-pump-

thaw technique. Solutions were typically 20 μM in the compound and deaerated through three cycles of freeze-pump-thaw.

All electrochemical experiments were executed in a home-built cylindrical vacuum-tight one-compartment cell. A spiral shaped Pt wire and an Ag wire as the counter and pseudoreference electrodes are sealed into glass capillaries and fixed by quickfit screws via standard joints. A platinum electrode is introduced as the working electrode through the top port via a Teflon screw cap with a suitable fitting. It is polished with first 1 μm and then 0.25 μm diamond paste before measurements. The cell may be attached to a conventional Schlenk line via a side arm equipped with a Teflon screw valve, allowing experiments to be performed under an argon atmosphere with approximately 5-7 mL of analyte solution. NBu_4PF_6 (0.1 mM) was used as the supporting electrolyte. Referencing was done with addition of an appropriate amount of decamethylferrocene (Cp^*_2Fe) as an internal standard to the analyte solution after all data of interest had been acquired. Representative sets of scans were repeated with the added standard. Electrochemical data were acquired with a computer-controlled BASi CV50 potentiostat. The optically transparent thin-layer electrochemical (OTTLE) cell was home-built and followed the design of Hartl et al.[2] It comprised a Pt working and counter electrode and a thin silver wire as a pseudoreference electrode sandwiched between two CaF_2 windows of a conventional liquid IR cell with the working electrode positioned in the center of the spectrometer beam.

Computational Details. The ground-state electronic structures were calculated by density functional theory (DFT) methods using the Gaussian 09[3] program package. Quantum-chemical studies were performed without any symmetry constraints. Open-shell systems were calculated by the unrestricted Kohn−Sham approach.[4] Geometry optimizations followed by vibrational analysis were performed either in a vacuum or in solvent media. The quasi-relativistic Wood−Boring small-core pseudopotentials (MWB),[5,6] the corresponding optimized set of basis functions[7] for platinum and the halogen atoms, and the 6-31G(d)-polarized double-ζ basis set[8] for the remaining atoms were employed together with the Perdew−Burke−Ernzerhof exchange and correlation functional (PBE0).[9,10] Solvent effects were accounted for by the polarizable conductor continuum model (PCM)[11-14] with standard parameters for dichloromethane. Absorption spectra and orbital energies were calculated using time-dependent DFT (TD-DFT)[15] with the same functional/basis set combinations as those mentioned above. For an easier comparison with the experiment, the obtained absorption and emission energies were converted into wavelengths and broadened by a Gaussian distribution (full width at half-maximum = 3000 cm^{-1}) using the program GaussSum.[16] Atomic coordinates of the calculated structures are provided in Tables Table S8 and Table S9.

Preparation of Compounds

1-Mercaptopyrene

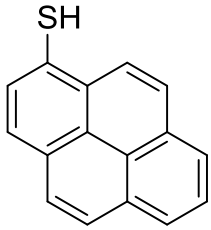

Original synthesis: In a Schlenk flask 503 mg (1.79 mmol) 1-bromopyrene were suspended in 20 ml of Et_2O and cooled to -78 °C. 1.1 ml (1.8 mmol, 1.6 M) of an *n*-buthyllithium solution in hexane were added dropwise. The solution was stirred at -78 °C for 1 h before the suspension was transferred into a cooled (-60 °C) dropping funnel. The solution of the lithiated pyrene was added dropwise to a solution of 248 mg (17.9 mmol) of SO_2Cl_2 in 20 ml of Et_2O, which was precooled to -78 °C. The solution was slowly warmed to r.t. overnight and the solvent was evaporated. A yellow powder was obtained.

The pyrene sulfonic acid chloride was dissolved in abs. toluene, filtered and added to a solution of 1.4 g (5.37 mmol) of PPh_3 in 20 ml of toluene. After stirring the yellow solution, containing some colorless solid, for 20 min at r.t. 10 ml of water were added and the solution was stirred for additional 10 min. The aqueous phase was discarded and the toluene phase was extracted with 10 x 20 ml of 1 M NaOH. The aqueous phase was washed with 2 x 10 ml of toluene, acidified with diluted HCl and extracted with 4 x 20 ml of CH_2Cl_2. The combined organic phases were dried over $MgSO_4$ and evaporated to dryness. Yield: 20 % (84 mg).

Alternative, improved synthesis: 275 mg (0.8 mmol) of 1-bromopyrene and 240 mg (3.42 mmol) of sodium methanethiolate were dissolved in DMF under nitrogen and heated to reflux for 2 h. 50 ml of 0.1 N HCl were added and the mixture was extracted with diethyl ether (3 x 50 ml). After washing the organic phase with water (2 x 50 ml), drying over $MgSO_4$ and removing all volatiles, the crude product was purified by column chromatography (petroleum ether / ethyl acetate, 5:1) to give the title compound as a yellow solid in 73 % yield (137 mg). ^{1}H NMR ($CDCl_3$, 399.79 MHz, 300 K): δ 8.37 (d, $^3J_{HH}$ = 9.2 Hz, 1H, H_{Aryl}), 8.18 (m, 2H, H_{Aryl}), 8.14 (d, $^3J_{HH}$ = 9.2 Hz, 1H, H_{Aryl}), 8.02 (m, 5H, H_{Aryl}), 3.85 (s, 1H, -S*H*). ^{13}C {^{1}H} NMR (150.93 MHz, DMSO-d_6, 300 K): δ 131.6, 131.1, 130.1, 129.6, 129.3, 128.0, 127.4, 127.2, 126.4, 125.7, 125.5, 125.4, 125.3, 125.0, 124.5, 124.4. Anal. Calcd for $C_{16}H_{10}S$: C, 82.02; H, 4.30; S, 13.68. Found: C, 81.94; H, 4.39; S, 12.65.

***trans*-Pt(bodipy)(PEt$_3$)$_2$(*S*-1-thiopyrene) (BPtSPyr)**

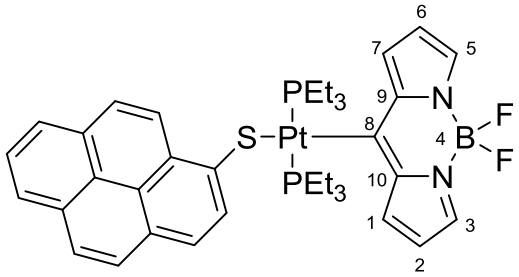

134 mg (172 µmol) of *trans*-Pt(bodipy)I(PEt$_3$)$_2$ (**BPtI**) and 49 mg (189 µmol) of AgOTf were dissolved in 0.5 ml of CD_2Cl_2 and heated to reflux for 10 min. After reaction control by ^{31}P NMR spectroscopy, all volatiles were removed and the solids were taken up in toluene and filtered. The filtered solution was poured into a toluene solution of 49 mg (207 µmol) of 1-mercaptopyrene and 38 µl (275 µmol) of $^{i}Pr_2NH$ and the mixture was stirred at r.t. for 1.5 h. All volatiles were removed, the crude solids were dissolved in benzene and the solution was filtered over Celite. After recrystallization from *n*-pentane / benzene 6:1, the product was obtained as a red crystalline solid. Yield: 60 % (88 mg). ^{1}H NMR (600.33 MHz, THF-*d8*, 298 K): δ 8.99 (d, $^3J_{HH}$ = 9.2 Hz, 1H, H$_{Pyr}$), 8.76 (d, $^3J_{HH}$ = 7.9 Hz, 1H, H$_{Pyr}$), 8.07 (d, $^3J_{HH}$ = 7.5 Hz, 1H, H$_{Pyr}$), 8.03 (m, 3H, H$_{Pyr}$), 7.92 (d, $^3J_{HH}$ = 8.8 Hz, 1H, H$_{Pyr}$), 7.89 (vt, $^3J_{HH}$ = 7.5 Hz, 1H, H$_{Pyr}$), 7.85 (d, $^3J_{HH}$ = 8.8 Hz, 1H, H$_{Pyr}$), 7.69 (br s, 2H, H3, H5), 7.65 (d, $^3J_{HH}$ = 3.9 Hz, 2H, H1, H7), 6.52 (dd, $^3J_{HH}$ = 3.9 Hz, $^3J_{HH}$ = 2.0 Hz, 2H, H2, H6), 1.78 (m, 12H, PC*H*$_2$CH$_3$), 1.01 (m, 18H, PCH$_2$C*H*$_3$). ^{13}C {^{1}H} NMR (150.97 MHz, THF-*d8*, 298 K): δ 188.0 (t, $^2J_{PC}$ = 8.3 Hz, with satellites J_{PtC} = 848 Hz, C8), 146.4 (s, with shoulders, C$_{Pyr}$), 144.4 (s with satellites, $^2J_{PtC}$ = 38.2 Hz, C9, C10), 138.0 (s, C3, C5), 133.6 (s with satellites, $^3J_{PtC}$ = 45.2 Hz, C1, C7), 133.2 (s, C$_{Pyr}$), 132.9 (s, C$_{Pyr}$), 132.4 (s, C$_{Pyr}$), 132.0 (s with satellites, J_{PtC} = 34.7 Hz, C$_{Pyr}$), 128.5 (s, C$_{Pyr}$), 128.1 (s, C$_{Pyr}$), 127.3 (s, C$_{Pyr}$), 126.9 (s, C$_{Pyr}$), 126.7 (s, C$_{Pyr}$), 126.6 (s, C$_{Pyr}$), 126.1 (s, C$_{Pyr}$), 126.0 (s, C$_{Pyr}$), 124.8 (s, C$_{Pyr}$), 124.7 (s, C$_{Pyr}$), 124.3 (s, C$_{Pyr}$), 116.6 (s, C2, C6), 14.8 (t, J_{PC} = 17.4 Hz, with satellites, $^2J_{PtC}$ = 23.6 Hz, P*C*H$_2$CH$_3$), 8.3 (s with shoulders, PCH$_2$*C*H$_3$). ^{31}P {^{1}H NMR (161.83 MHz, THF-*d8*, 300 K): δ 6.84 (s with satellites, J_{PtP} = 2484 Hz). ^{195}Pt {^{1}H} NMR (85.55 MHz, THF-*d8*, 300 K): δ -4378 (t, J_{PtP} = 2484 Hz). Anal. Calcd for $C_{37}H_{45}BF_2N_2P_2PtS$: C, 51.94; H, 5.30; N, 3.22; S, 3.75. Found: C, 51.96; H, 5.19; N, 3.59; S, 2.69.

***cis*/*trans*-PtBr(mesityl)(PEt_3) (*cis*/*trans*-MesPtBr)**

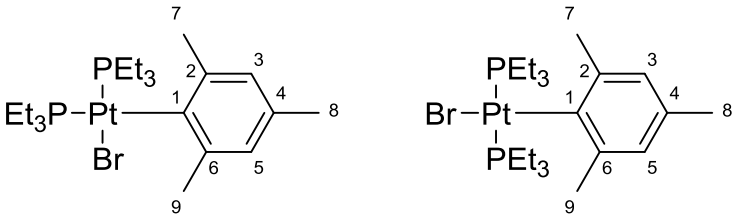

In a Young-tube 98 mg (200 µmol) of $Pt(Et)_2(PEt_3)_2$ were dissolved in 0.5 ml of C_6D_6 and placed under vacuum before heating to 115°C for 45 min. The progress of the reaction was controlled by ^{31}P NMR spectroscopy. After conversion to $Pt(PEt_3)_2(\eta^2\text{-}C_2H_4)$ was complete, 34 µl (220 µmol) of degassed mesityl bromide in 0.5 ml of C_6D_6 were added. The mixture was placed under vacuum again and then heated to 110 °C for 7 h. On addition of 4 ml of *n*-pentane 10 mg of pure ***cis*-MesPtBr** crystallized from the solution. From the remaining solution all volatiles were removed and the remaining solid was washed with 2 x 1 ml of *n*-pentane. This fraction contained slightly impure ***trans*-MesPtBr** with about 3 % of the *cis*-isomer. Overall yield: 51 % (64 mg). ***cis*-MesPtBr**: ^1H NMR (399.79 MHz, $CDCl_3$, 300 K): δ 6.63 (s, 2H, H3, H5), 2.46 (s, 6H, H7, H9), 2.18 (s, 3H, H8), 2.06 (m, 6H, PCH_2CH_3), 1.64 (m, 6H, PCH_2CH_3), 1.17 (m, 9H, PCH_2CH_3), 1.03 (m, 9H, PCH_2CH_3). ^{13}C {^1H} NMR (100.54 MHz, $CDCl_3$, 300 K): δ 150.6 (dd, $^2J_{PC}$ = 110 Hz, $^2J_{PC}$ = 7.4 Hz, C1), 141.4 (vt, $^3J_{PC}$ = 1.6 Hz, C2, C6), 132.3 (s, C4), 127.6 (d, with shoulders, $^4J_{PC}$ = 7.1 Hz, C3, C5), 26.3 (d, with satellites, $^4J_{PC}$ = 3.0 Hz, $^3J_{PtC}$ = 53.1 Hz, C7, C9), 21.0 (s, C8), 18.3 (dd, with satellites, J_{PC} = 37.4 Hz, $^3J_{PC}$ = 3.0 Hz, $^2J_{PtC}$ = 57.4 Hz, PCH_2CH_3), 15.5 (d, with satellites, J_{PC} = 26.5 Hz, $^2J_{PtC}$ = 18 Hz, PCH_2CH_3), 8.6 (d, with satellites, $^2J_{PC}$ = 3.0 Hz, $^3J_{PtC}$ = 32.0 Hz, PCH_2CH_3), 8.4 (s, with satellites, $^3J_{PtC}$ = 14.0 Hz, PCH_2CH_3). ^{31}P {^1H NMR} (161.84 MHz, $CDCl_3$, 300 K): δ 8.19 (d, with satellites, $^2J_{PP}$ = 16.6 Hz, J_{PtP} = 1615 Hz), 0.7 (d, with satellites, $^2J_{PP}$ = 16.6 Hz, J_{PtP} = 4272 Hz). ^{195}Pt {^1H} NMR (85.56 MHz, $CDCl_3$, 300 K): δ -4488 (dd, J_{PtP} = 4272 Hz, 1615 Hz). ***trans*-MesPtBr**: ^1H NMR (399.79 MHz, $CDCl_3$, 300 K): δ 6.58 (s, with satellites, $^4J_{PtH}$ = 14.6 Hz, 2H, H3, H5), 2.47 (s, with shoulders, 6H, H7, H9), 2.16 (s, 3H, H8), 1.67 (m, 12H, PCH_2CH_3), 1.04 (m, 18H, PCH_2CH_3). ^{13}C {^1H} NMR (100.54 MHz, $CDCl_3$, 300 K): δ 140.2 (vt, $^3J_{PC}$ = 2.2 Hz, C2, C6), 135.7 (s, C1), 132.0 (br s, C4), 126.7 (s, with satellites, $^3J_{PtC}$ = 50.5 Hz, C3, C5), 27.3 (s, with satellites, $^3J_{PtC}$ = 88.8 Hz, C7, C9), 20.7 (s, C8), 15.4 (m, PCH_2CH_3), 8.4 (s, with satellites, $^3J_{PtC}$ = 24.4 Hz, PCH_2CH_3). ^{31}P {^1H} NMR (161.84 MHz, $CDCl_3$, 300 K): δ 9.32 (s, with satellites, J_{PtP} = 2791 Hz). ^{195}Pt {^1H} NMR (85.56 MHz, $CDCl_3$, 300 K): δ -4409 (t, J_{PtP} = 2791 Hz). Anal. Calcd for $C_{21}H_{41}BrP_2Pt$: C, 40.01; H, 6.55. Found: C, 40.35; H, 6.51.

***trans*-Pt(mesityl)(PEt_3)$_2$(*S*-1-thiopyrene) (MesPtSPyr)**

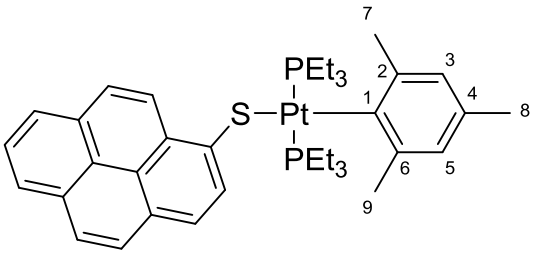

Under an atmosphere of nitrogen 104 mg (73 µmol) of **MesPtBr** and 18 mg (70 µmol) of AgOTf were dissolved in 0.5 ml CD_2Cl_2 and heated to reflux for 20 min. After reaction control by ^{31}P NMR spectroscopy indicated complete conversion to the triflato complex the solvent was removed. The solid residue was re-dissolved in 5 ml of toluene and filtered. This solution was added to a mixture containing 18 mg (76 µmol) of 1-mercaptopyrene and 20 µl (126 µmol) of $^{i}Pr_2NH$ in 5 ml of toluene. After 10 min of stirring at r.t. all volatiles were removed and the solid was purified by column chromatography (silica, petrol ether/NEt_3 30:1, R_f = 0.35). The product was obtained as a bright yellow solid in 76 % (37 mg) yield. ^1H NMR (399.79 MHz, $CDCl_3$, 300 K): δ 9.02 (d, $^3J_{HH}$ = 9.2 Hz, 1H, H_{pyr}), 8.74 (d, with shoulders, $^3J_{HH}$ = 8.0 Hz, 1H, H_{pyr}), 8.00 (dd, $^3J_{HH}$ = 7.6 Hz, $^4J_{HH}$ = 1.6 Hz, 1H, H_{pyr}), 7.95 (m, 2H, H_{pyr}), 7.83 (m, 3H, H_{pyr}), 7.76 (d, $^3J_{HH}$ = 8.9 Hz, 1H, H_{pyr}), 6.67 (s, with satellites, $^4J_{PtH}$ = 10.9 Hz, 1H, H3, H5), 2.66 (s, with shoulders, 6H, H7, H9), 2.17 (s, 3H, H8), 1.66 (m, 12H, P$CH_2$$CH_3$), 0.97 (m, 18H, PCH_2CH_3). ^{13}C {^1H} NMR (150.97 MHz, THF-*d8*, 298 K): δ 149.2 (s, with satellites, $^3J_{PtC}$ = 13.7 Hz, C_{pyr}), 144.8 (t, $^2J_{PC}$ = 9.0 Hz, with satellites, J_{PtC} = 864 Hz, C1), 141.9 (t, $^3J_{PC}$ = 1.8 Hz, with shoulders, C2, C6), 133.4 (s, C_{pyr}), 133.1 (s, C_{pyr}), 132.6 (s, C4), 132.4 (s, C_{pyr}), 132.0 (s, with satellites, $^4J_{PtC}$ = 35.2 Hz, C_{pyr}), 128.6 (s, C_{pyr}), 128.1 (s, with satellites, $^3J_{PtC}$ = 39.8 Hz, C3, C5), 128.0 (s, C_{pyr}), 127.3 (s, C_{pyr}), 126.5 (s, C_{pyr}), 126.4 (s, C_{pyr}), 126.3 (s, C_{pyr}), 126.1 (s, C_{pyr}), 124.7 (s, C_{pyr}), 124.2 (s, C_{pyr}), 124.1 (s, C_{pyr}), 124.0 (s, C_{pyr}), 28.0 (s, with satellites, $^3J_{PtC}$ = 78.7 Hz, C7, C9), 21.1 (s, C8), 15.8 (t, J_{PC} = 16.9 Hz, with satellites, $^2J_{PtC}$ = 34.9 Hz, PCH_2CH_3), 8.3 (s, with satellites, $^3J_{PtC}$ = 19.9 Hz, PCH_2CH_3). ^{31}P {^1H} NMR (161.84 MHz, THF-*d8*, 300 K): δ 6.96 (s, with satellites, J_{PtP} = 2734 Hz). ^{195}Pt {^1H} NMR (85.56 MHz, $CDCl_3$, 300 K): δ -4494 (t, J_{PtP} = 2734 Hz). Anal. Calcd for $C_{37}H_{50}P_2PtS$: C, 56.69; H, 6.43; S, 4.09. Found: C, 55.70; H, 6.66; S, 3.08.

NMR Spectroscopy

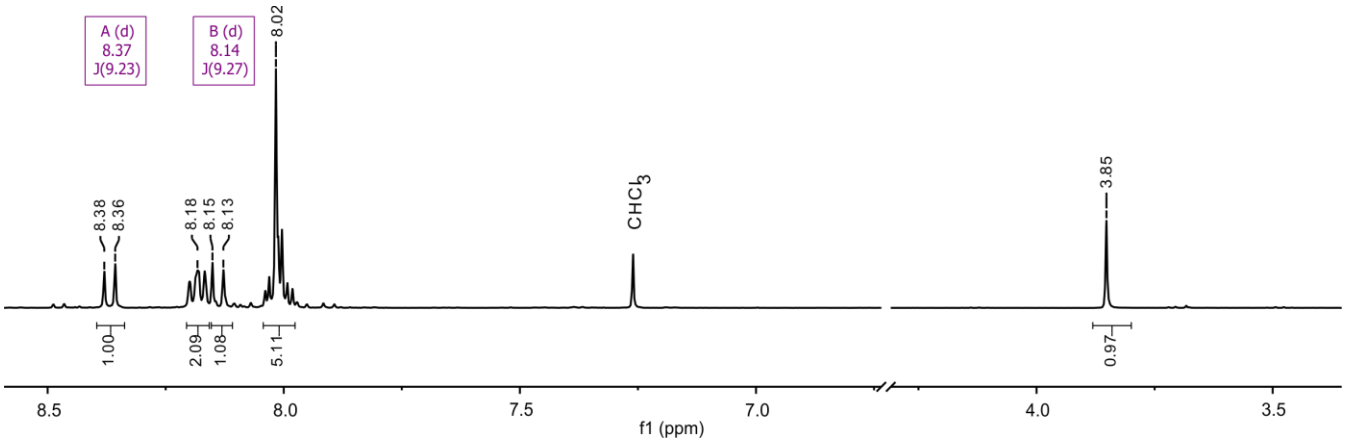

Figure S1. [1]H NMR spectrum of 1-mercaptopyrene in CDCl3.

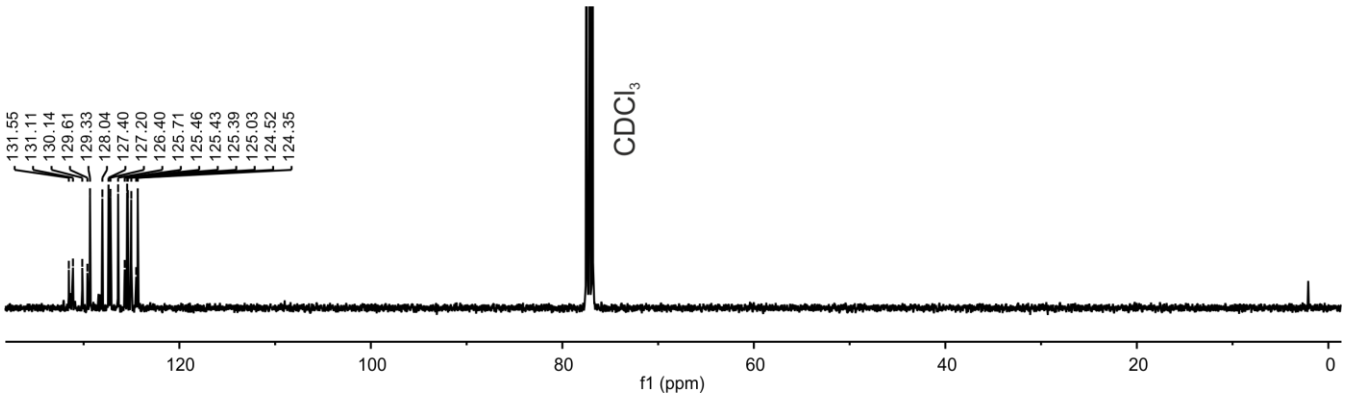

Figure S2. [13]C NMR spectrum of 1-mercaptopyrene in $CDCl_3$.

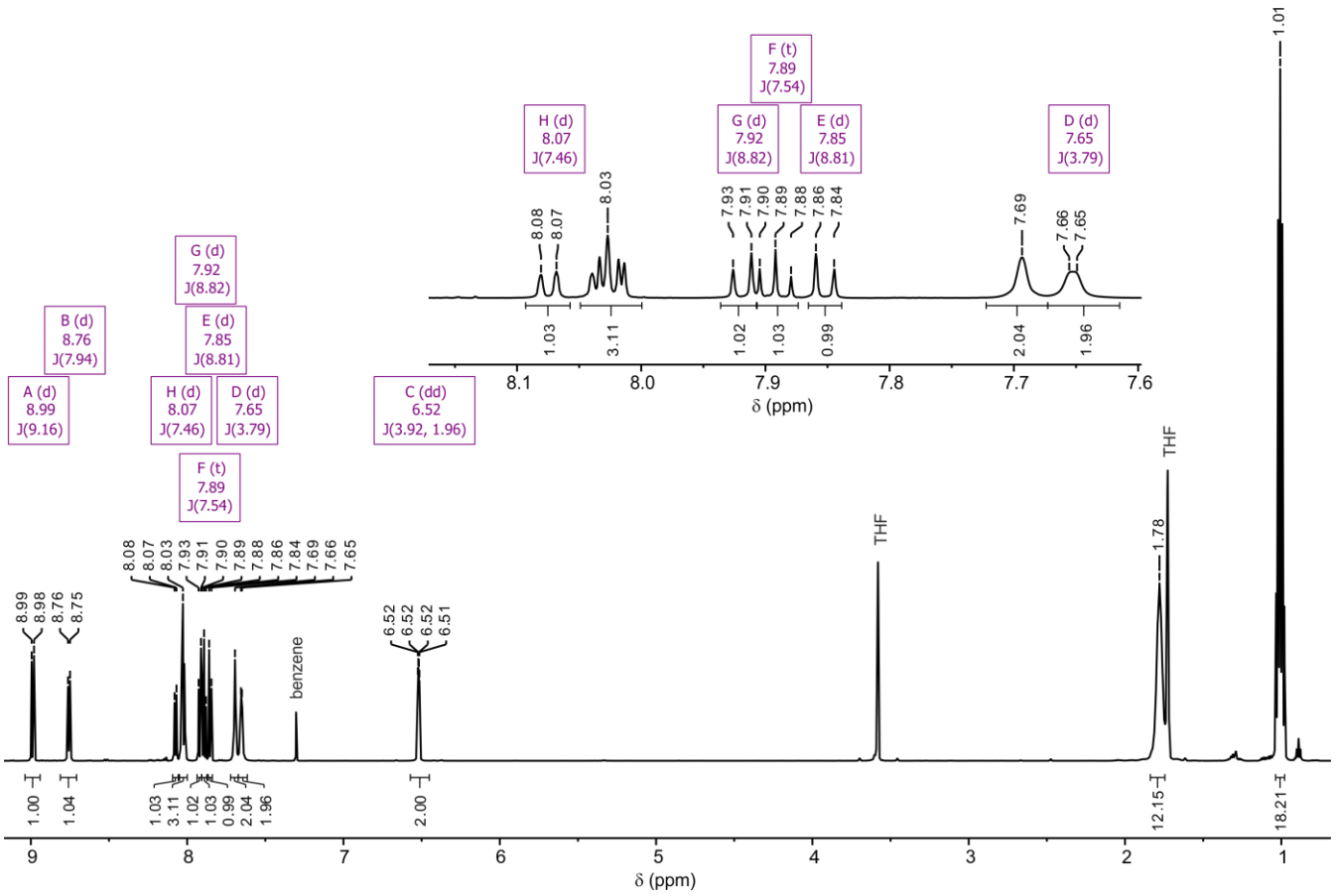

Figure S3. ^{1}H NMR spectrum of **BPtSPyr** in THF-*d8*.

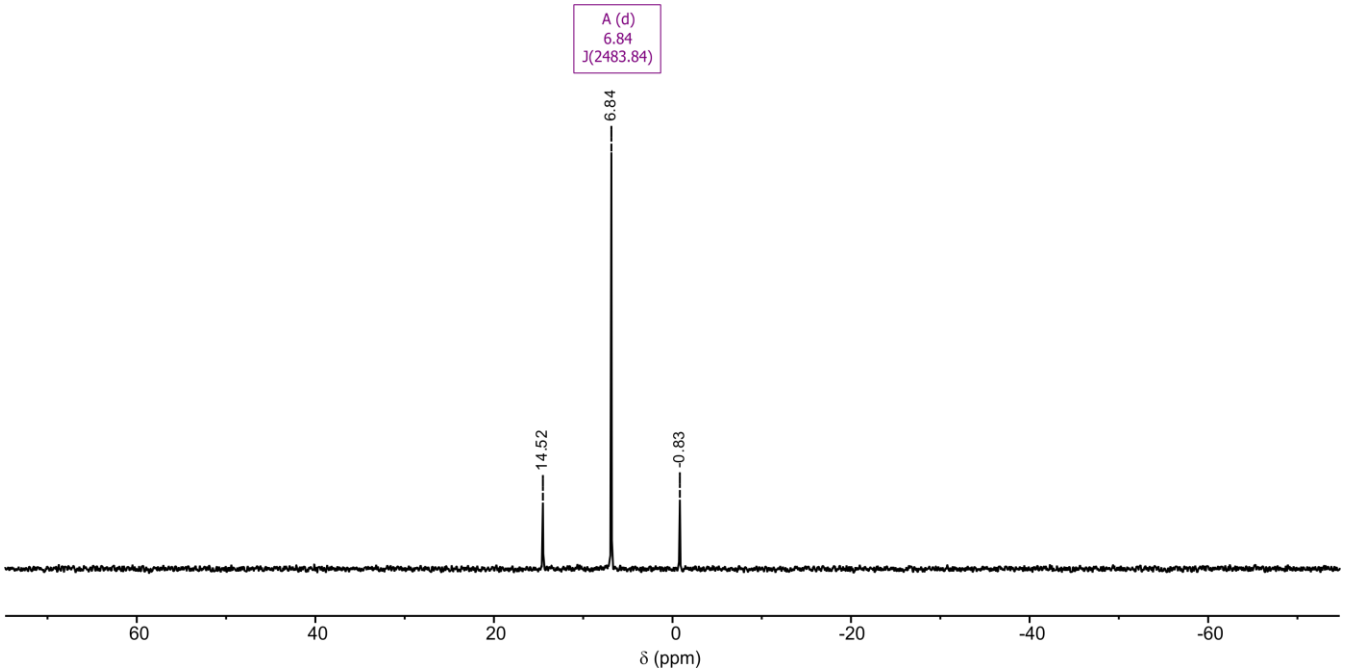

Figure S4. ^{31}P{^{1}H} NMR spectrum of **BPtSPyr** in THF-*d8*.

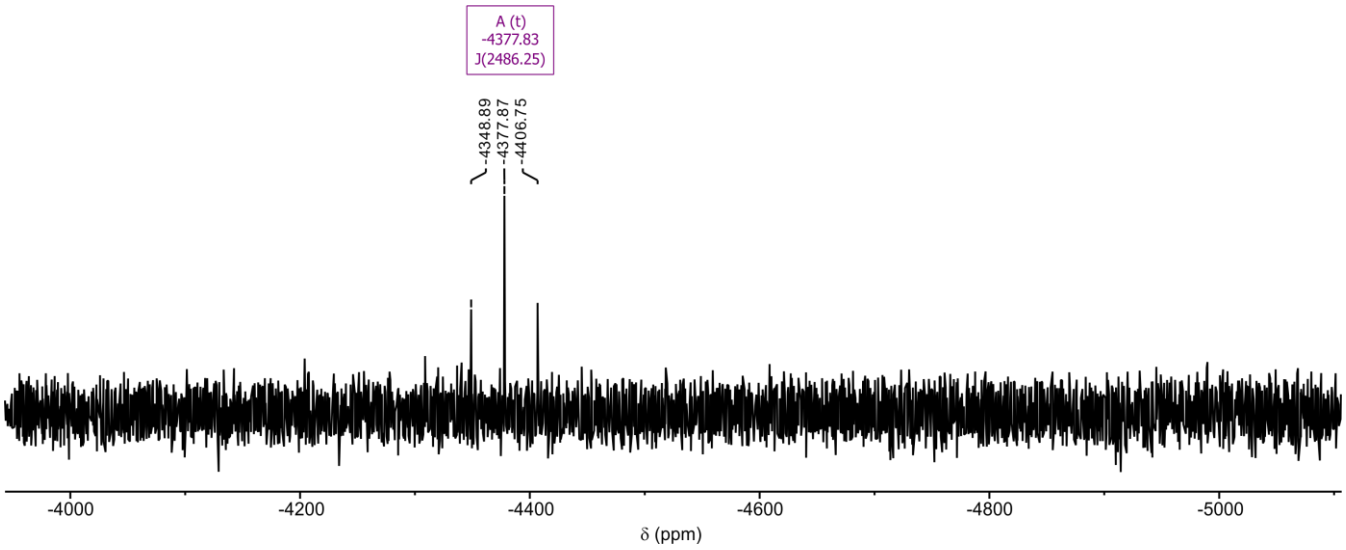

Figure S5. $^{195}Pt\{^{1}H\}$ NMR spectrum of **BPtSPyr** in THF-*d8*.

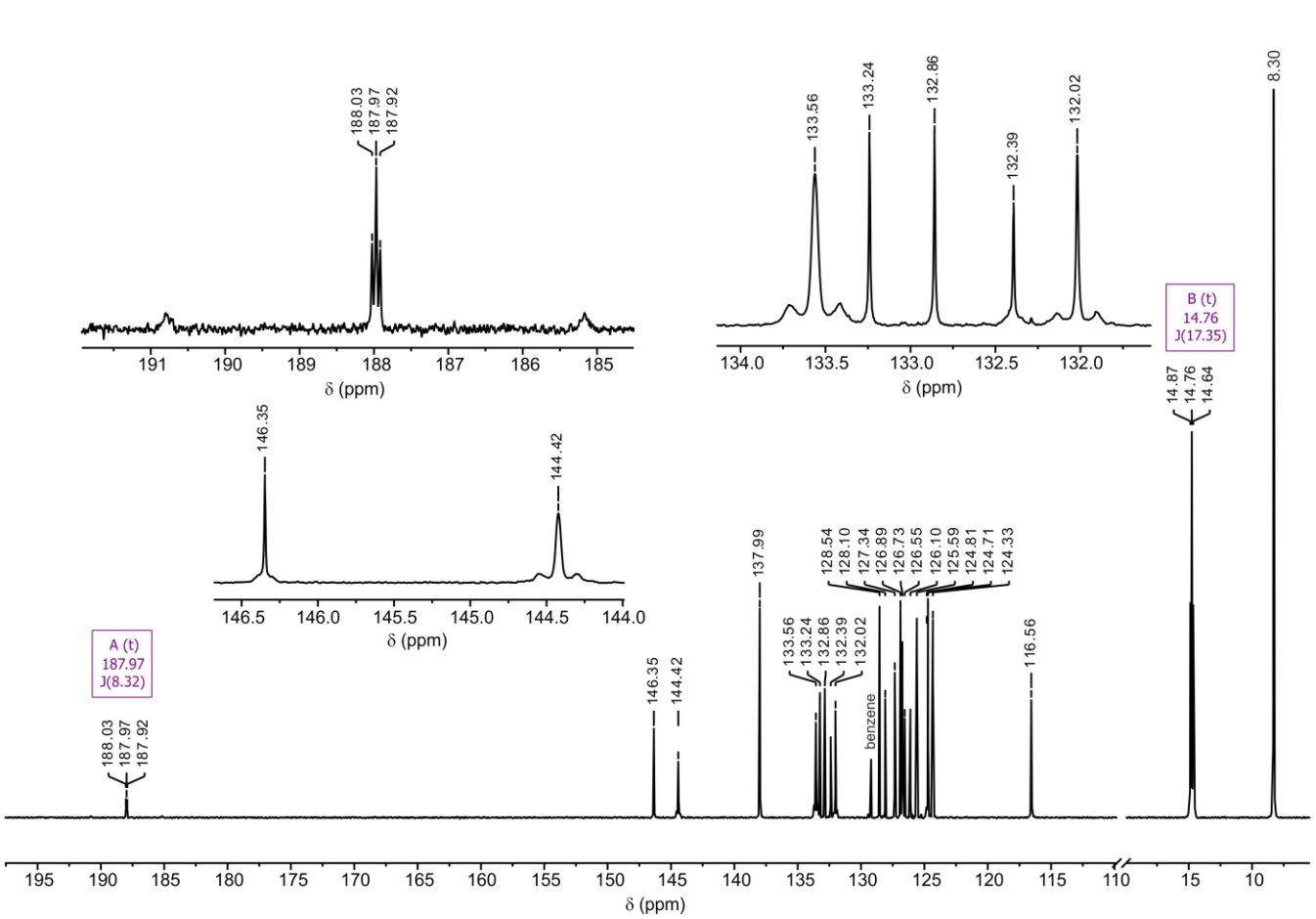

Figure S6. $^{13}C\{^{1}H\}$ NMR spectrum of **BPtSPyr** in THF-*d8*.

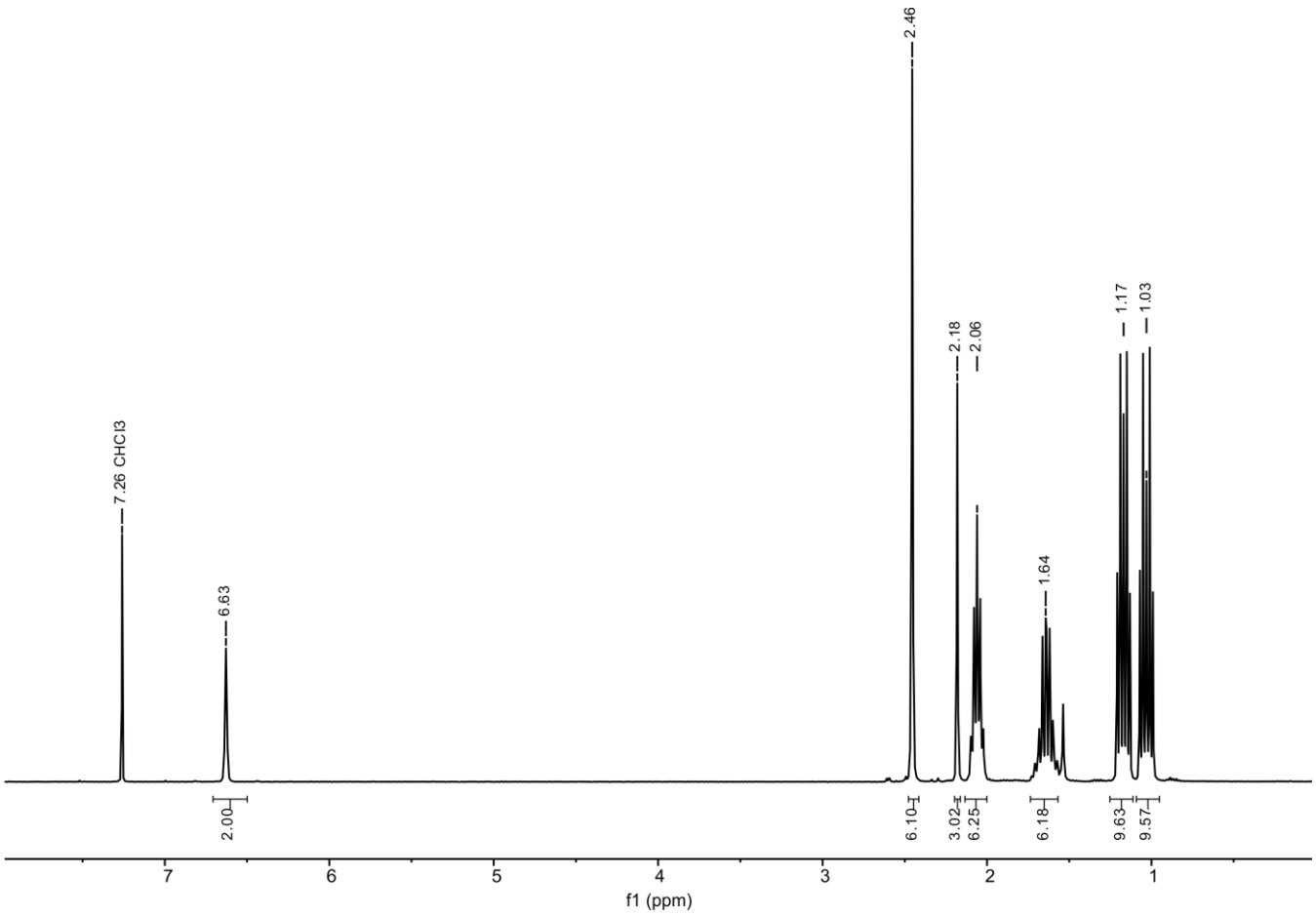

Figure S7. ^{1}H NMR spectrum of ***cis*-MesPtBr** in $CDCl_3$.

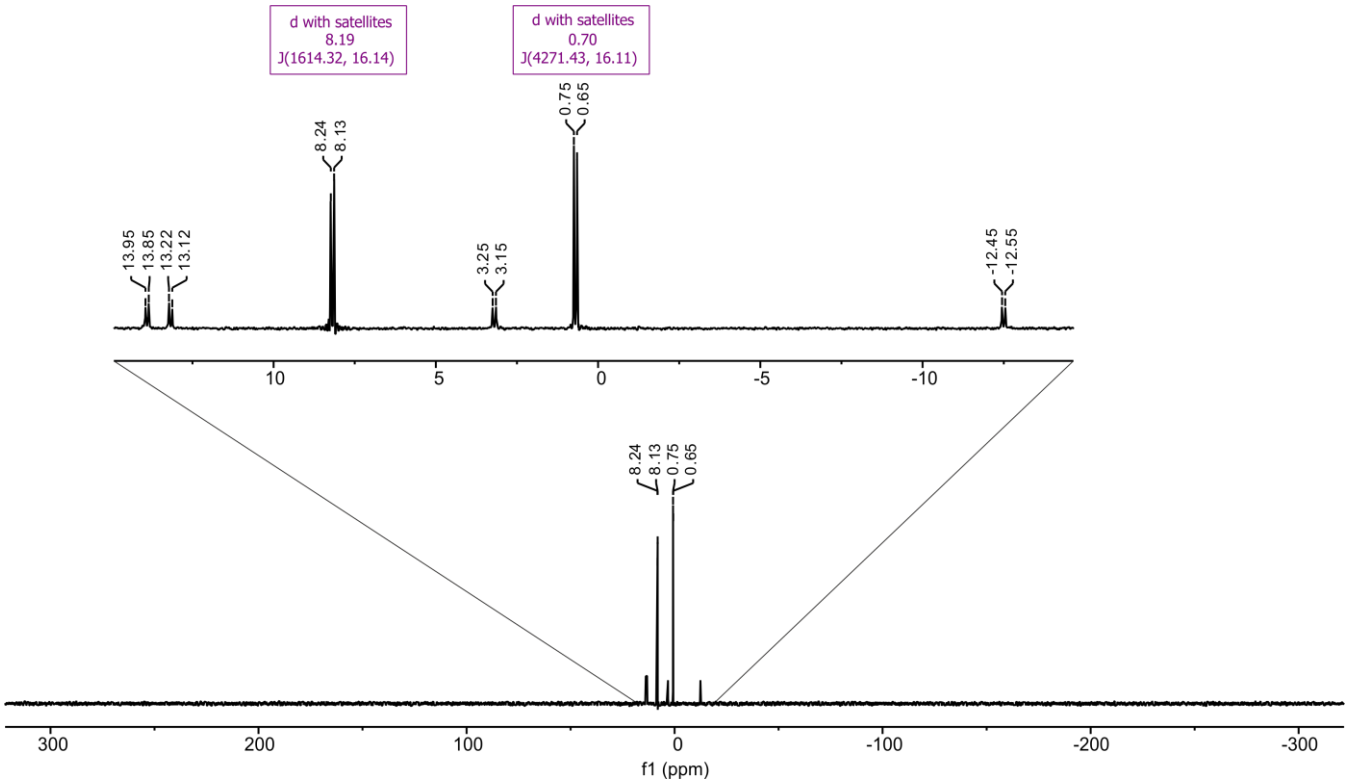

Figure S8. ^{31}P NMR spectrum of ***cis*-MesPtBr** in $CDCl_3$.

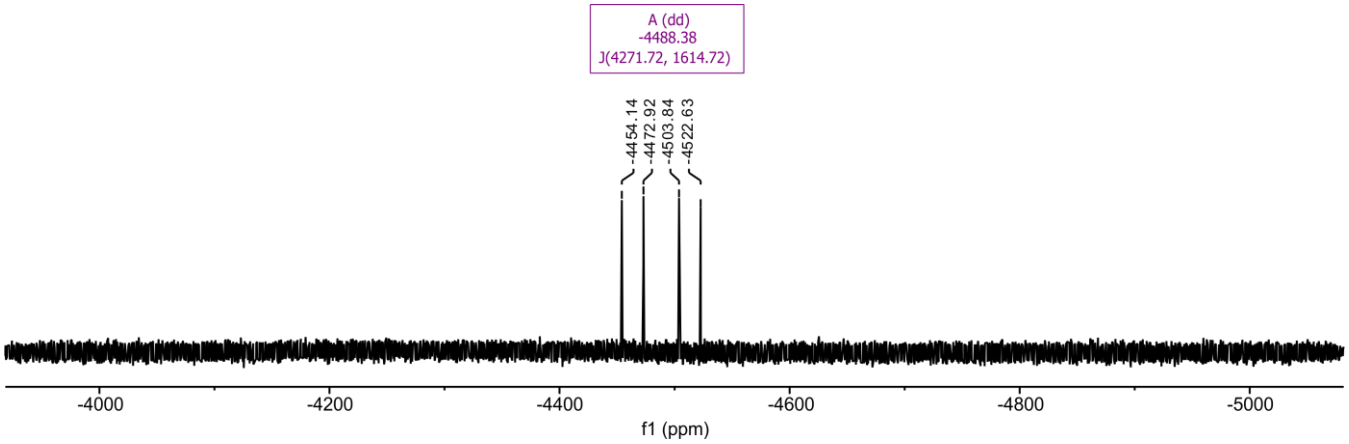

Figure S9. ^{195}Pt NMR spectrum of ***cis*-MesPtBr** in $CDCl_3$.

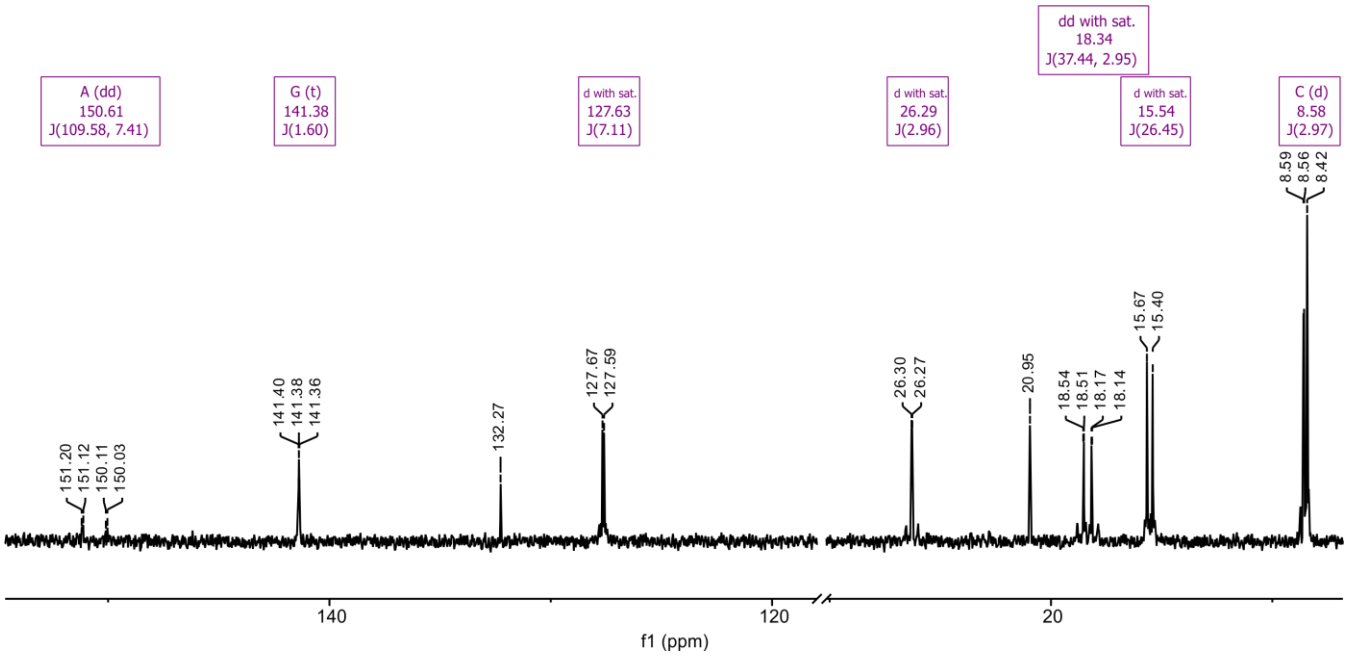

Figure S10. ^{13}C NMR spectrum of ***cis*-MesPtBr** in $CDCl_3$.

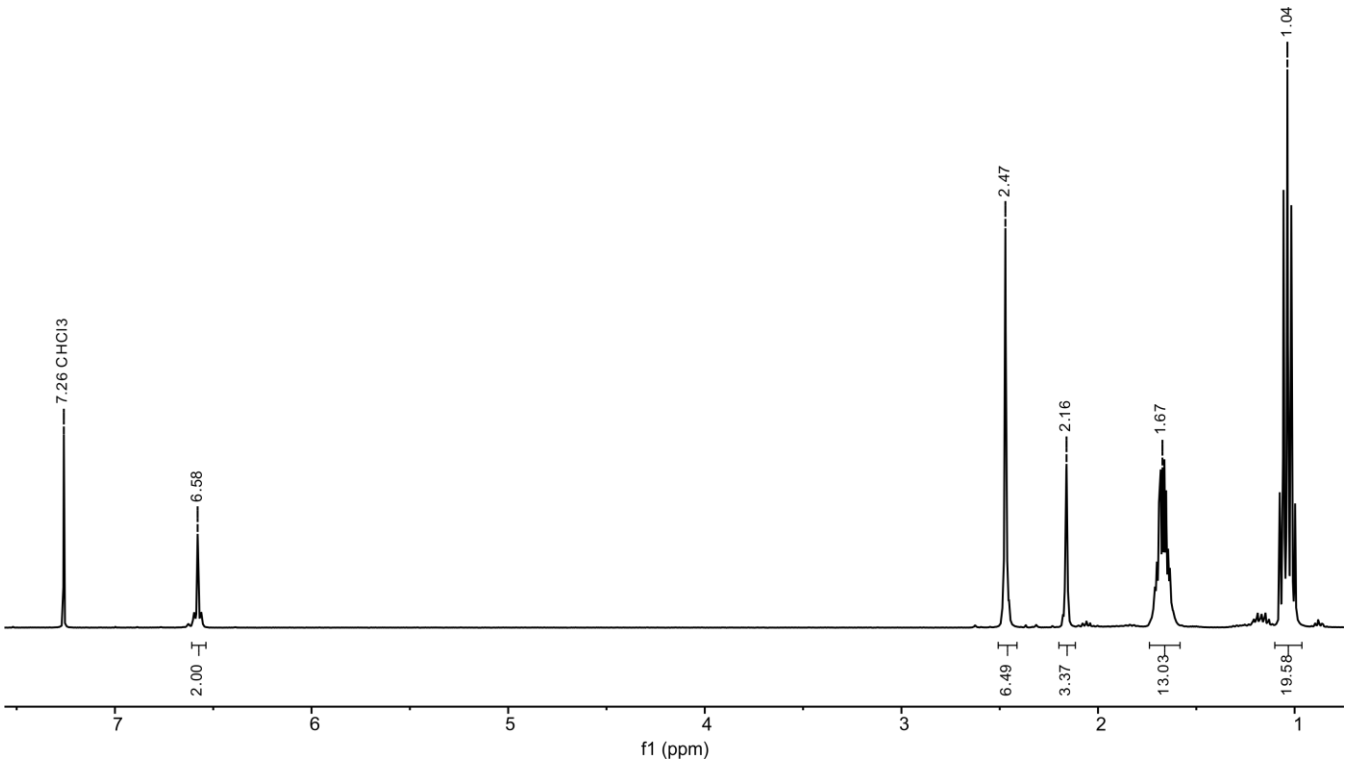

Figure S11. ^{1}H NMR spectrum of ***trans*-MesPtBr** in $CDCl_3$.

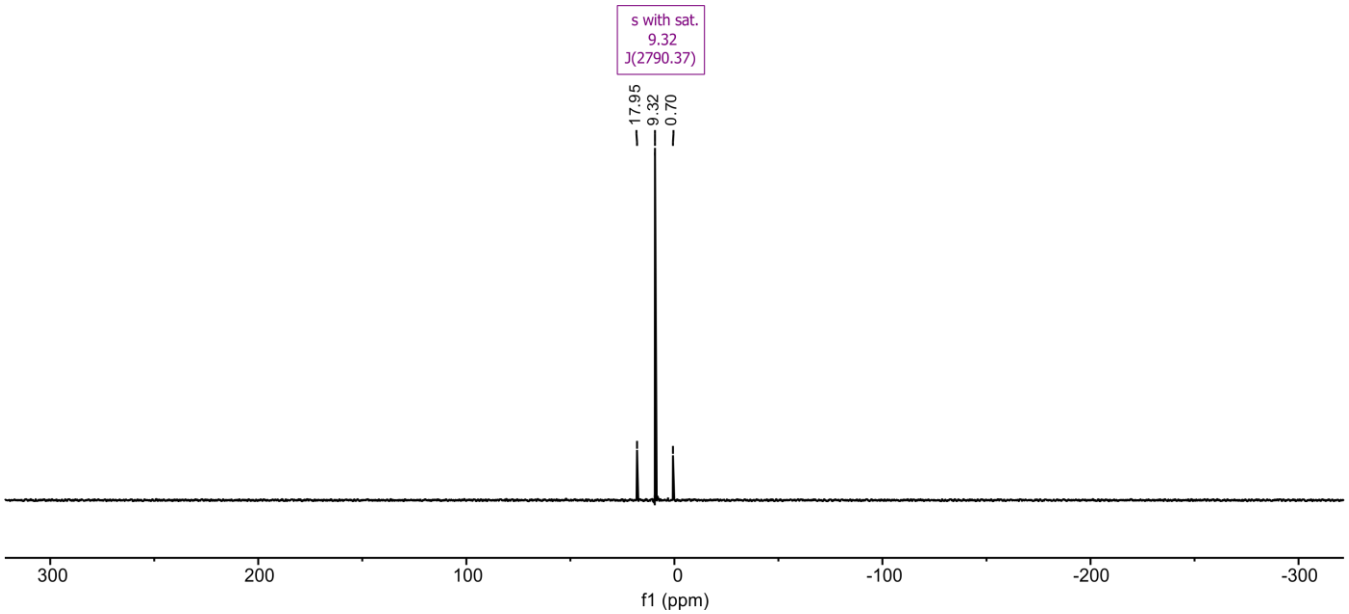

Figure S12. ^{31}P NMR spectrum of ***trans*-MesPtBr** in $CDCl_3$.

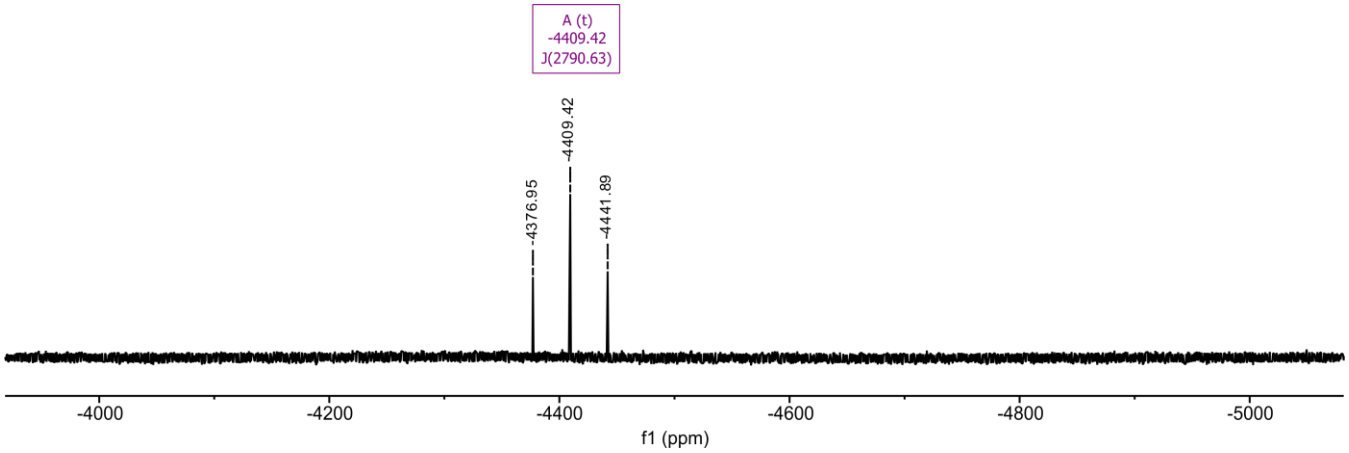

Figure S13. ^{195}Pt NMR spectrum of ***cis*-MesPtBr** in $CDCl_3$.

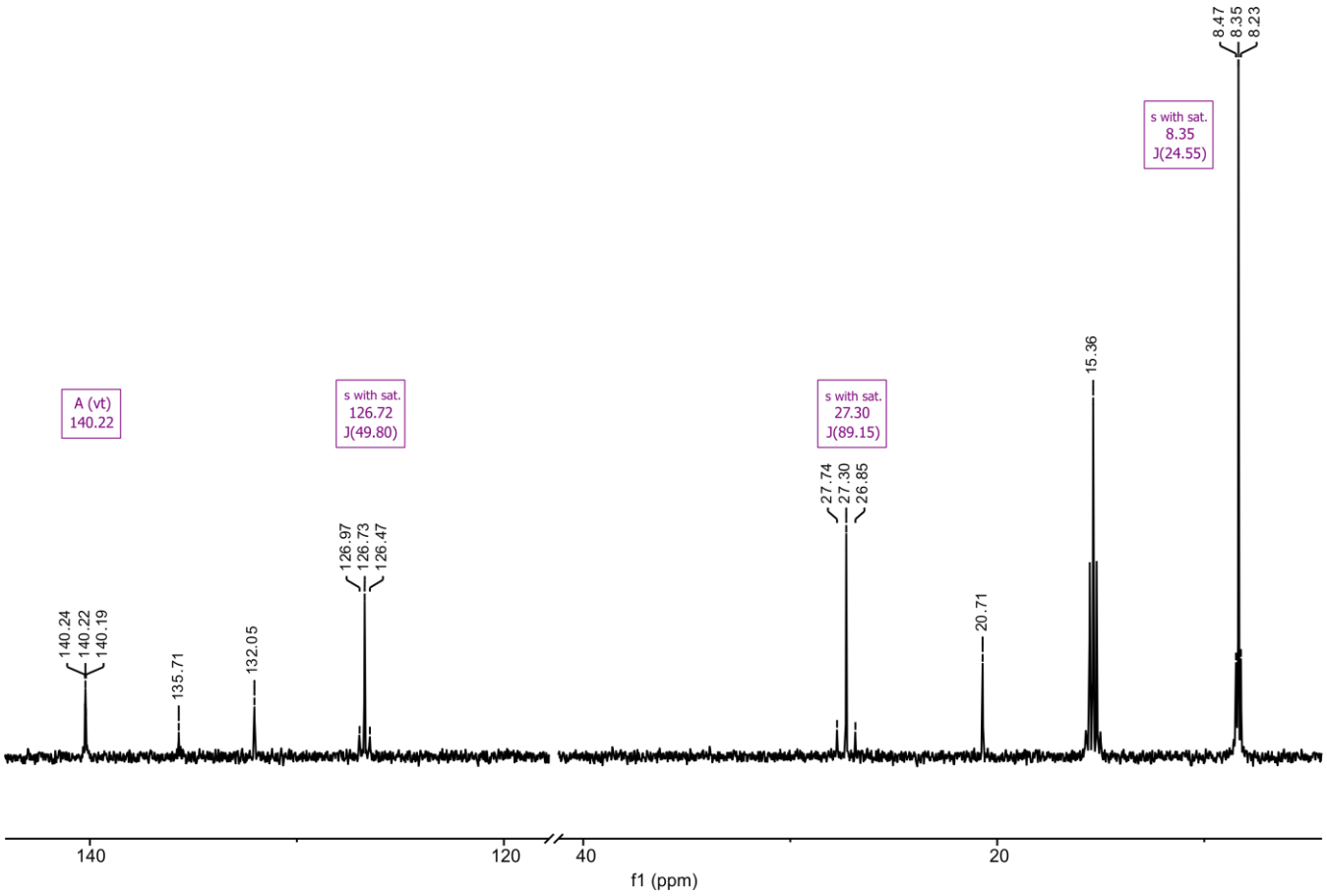

Figure S14. ^{13}C NMR spectrum of ***trans*-MesPtBr** in $CDCl_3$.

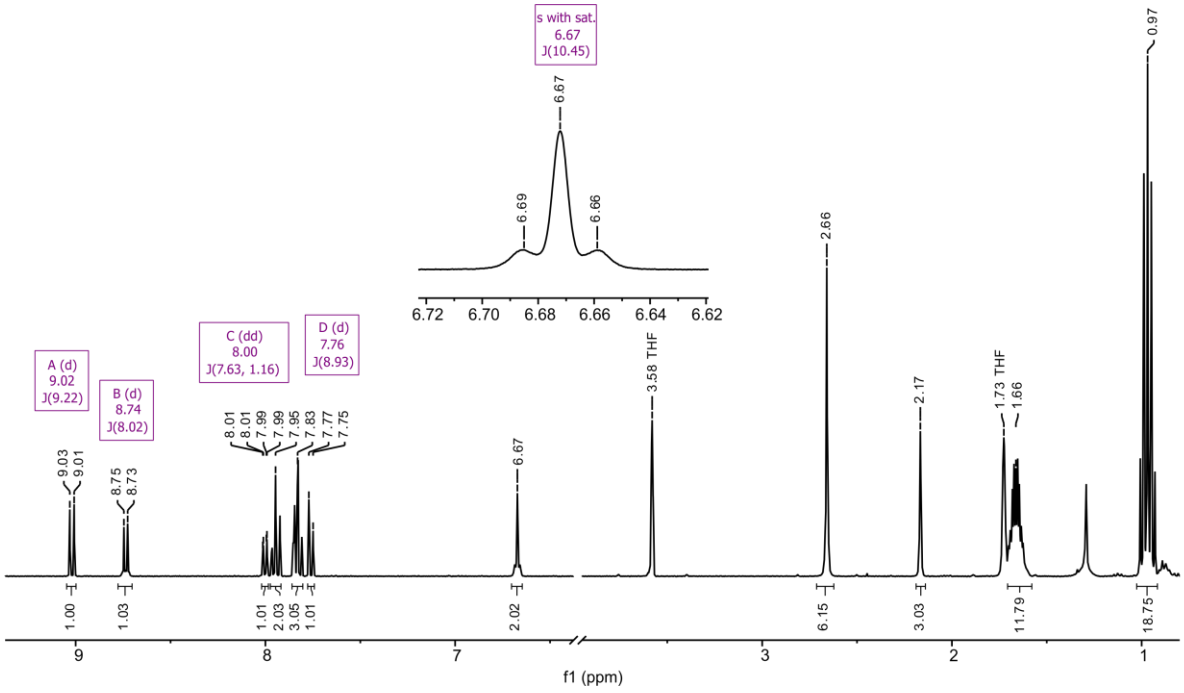

Figure S15. ^{1}H NMR spectrum of **MesPtSPyr** in THF-*d8*.

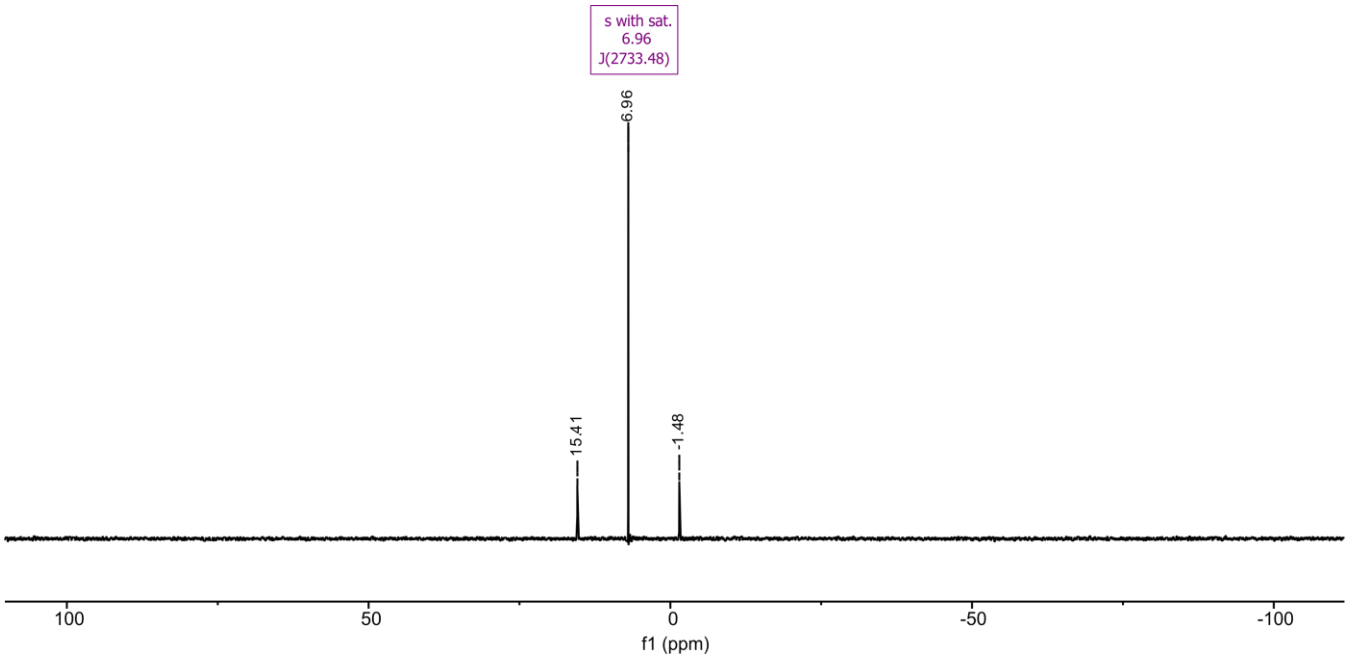

Figure S16. ^{31}P NMR spectrum of **MesPtSPyr** in THF-*d8*.

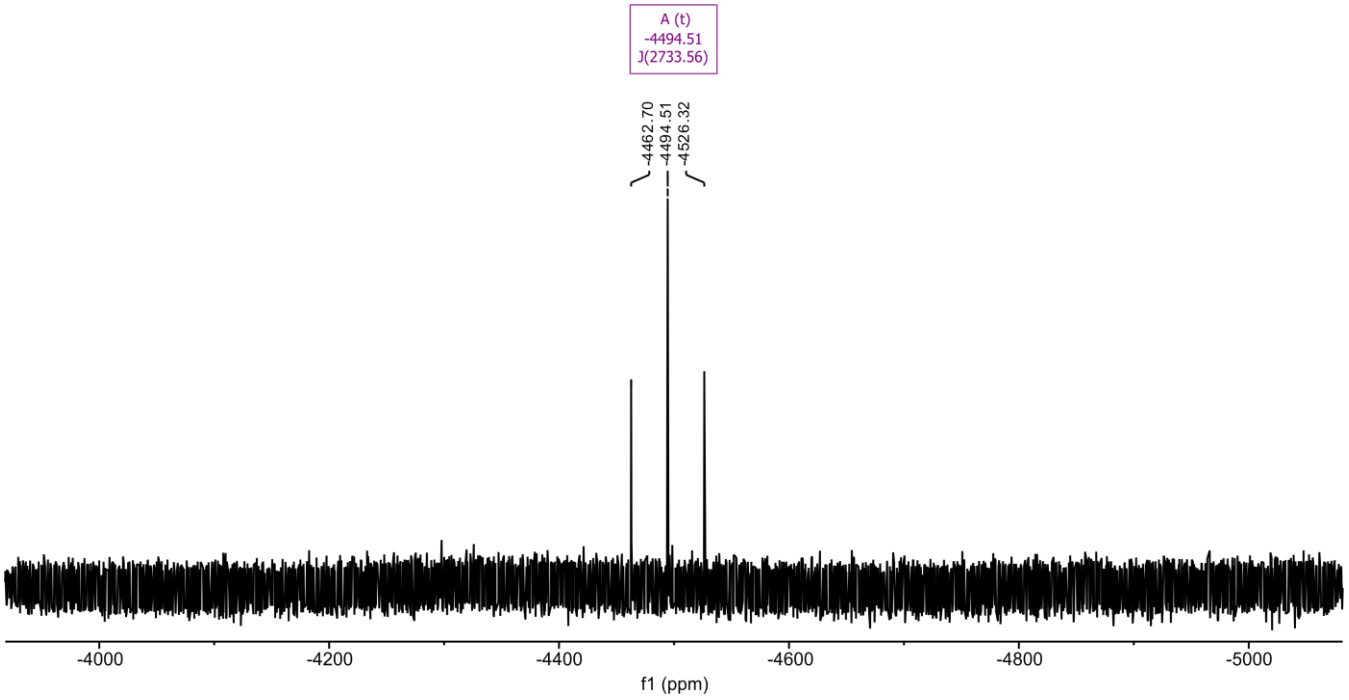

Figure S17. ^{195}Pt NMR spectrum of **MesPtSPyr** in THF-*d8*.

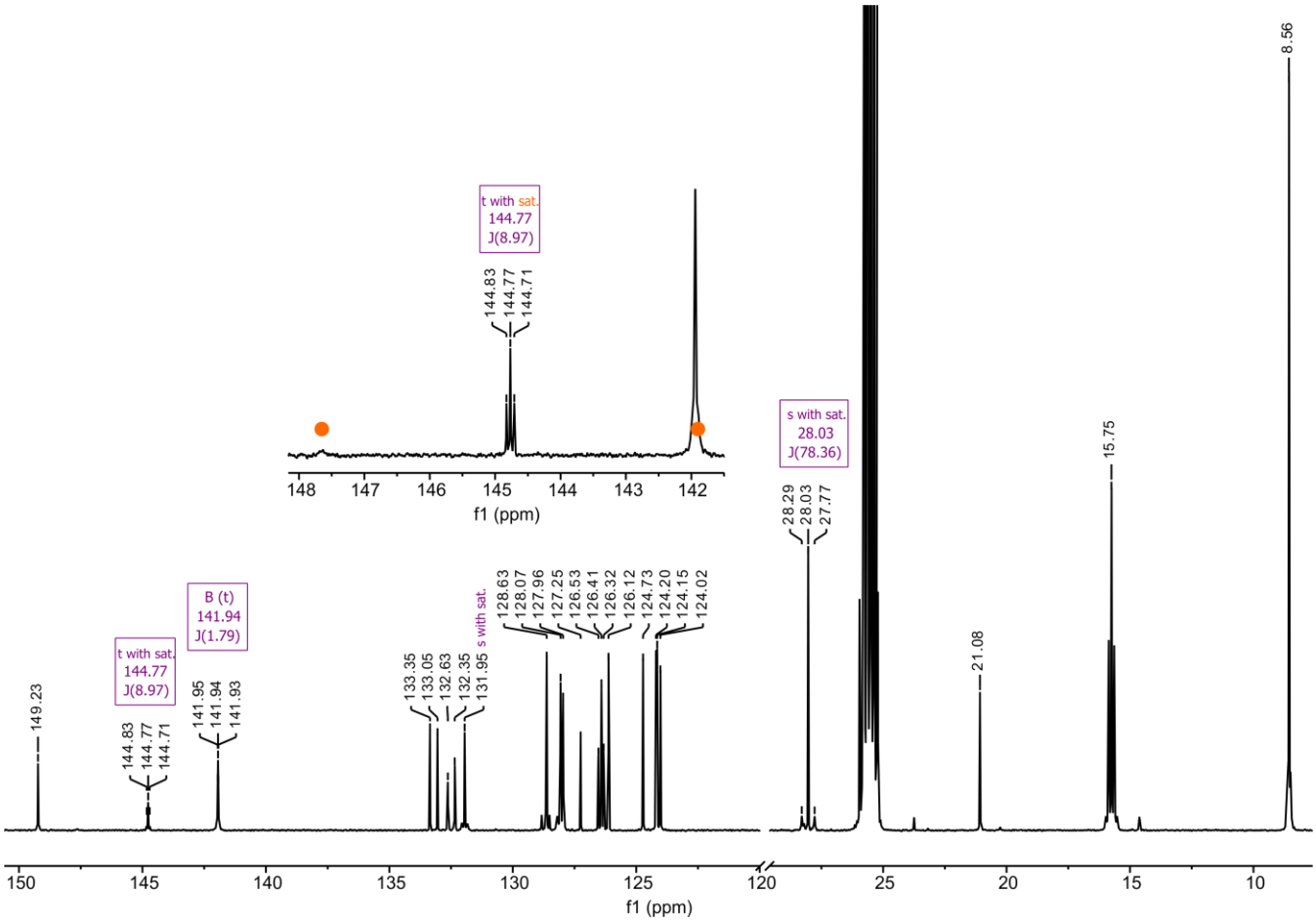

Figure S18. ^{13}C NMR spectrum of **MesPtSPyr** in THF-*d8*.

Emission Spectroscopy of MesPtSPyr

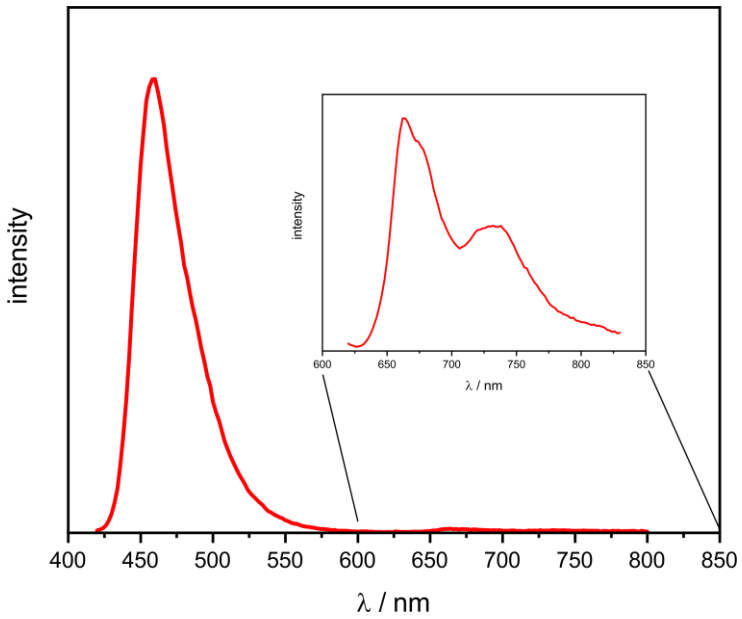

Figure S19. Emission of **MesPtSPyr** in a ca 1 μM degassed toluene solution at r.t.

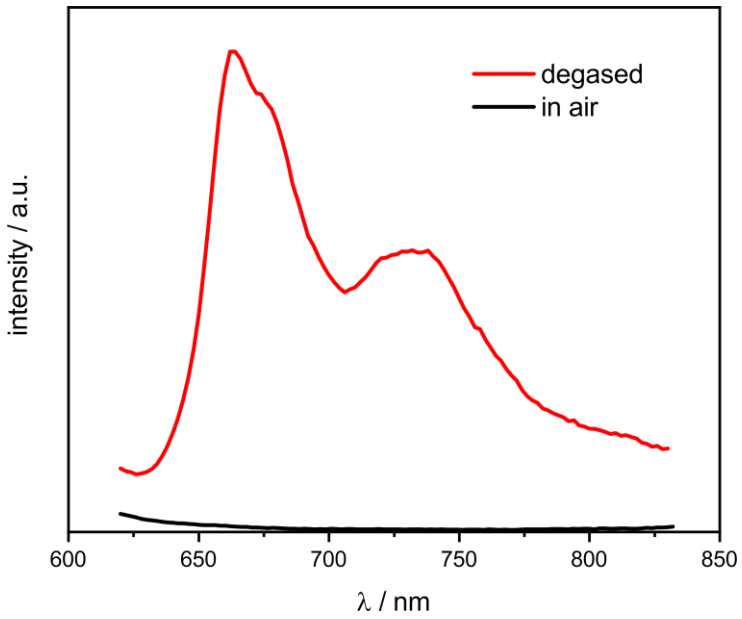

Figure S20. Phosphorescence emission of **MesPtSPyr** in a ca 1 μM toluene solution at r.t.

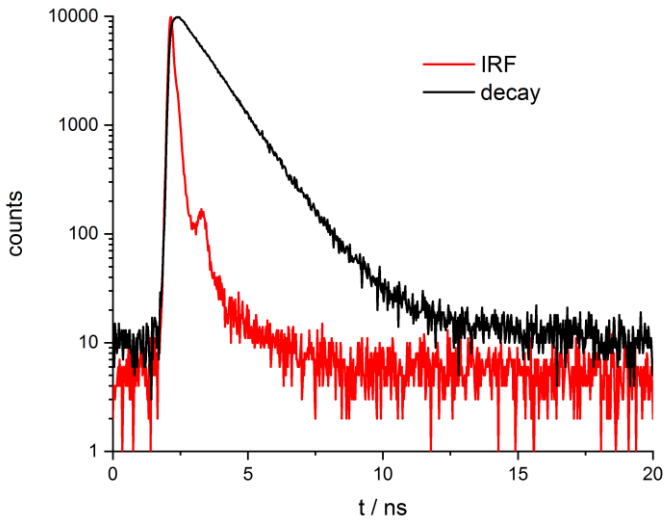

Figure S21. Fluorescence decay traces of **MesPtSPyr** in a deaerated and nitrogen-saturated 1 μM toluene solution at r.t. Decay can be fitted as a monoexponential decay with a lifetime of 1.113 ± 0.005 ns.

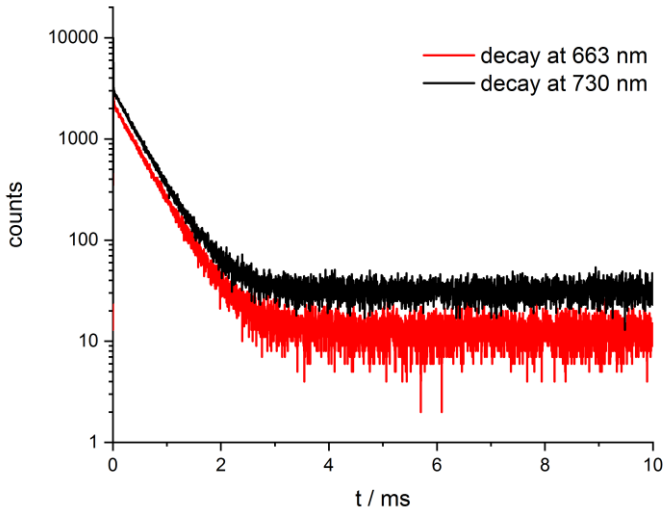

Figure S22. Phosphorescence decay traces of **MesPtSPyr** in a deaerated and nitrogen-saturated 1 μM toluene solution at r.t. Decay can be fitted as a monoexponential decay with a lifetime of 448 ± 6 μs.

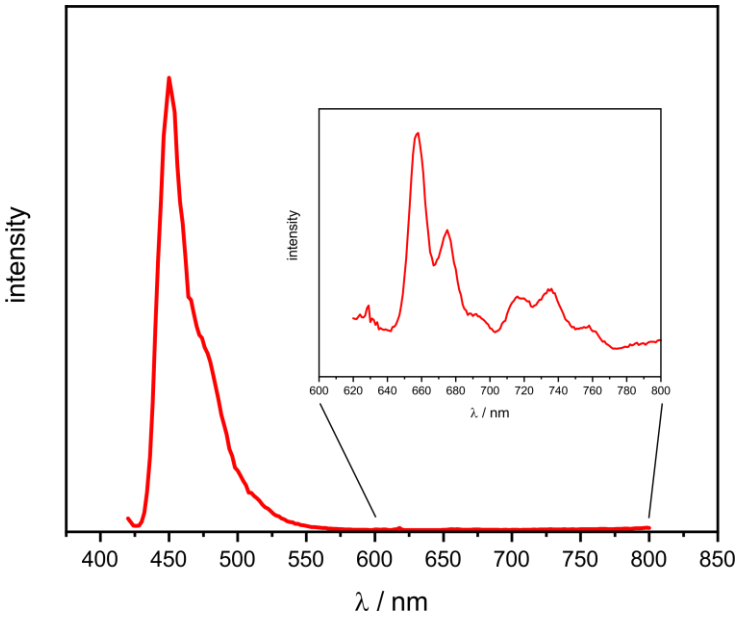

Figure S23. Emission of **MesPtSPyr** in a 2-MeTHF matrix at 77K.

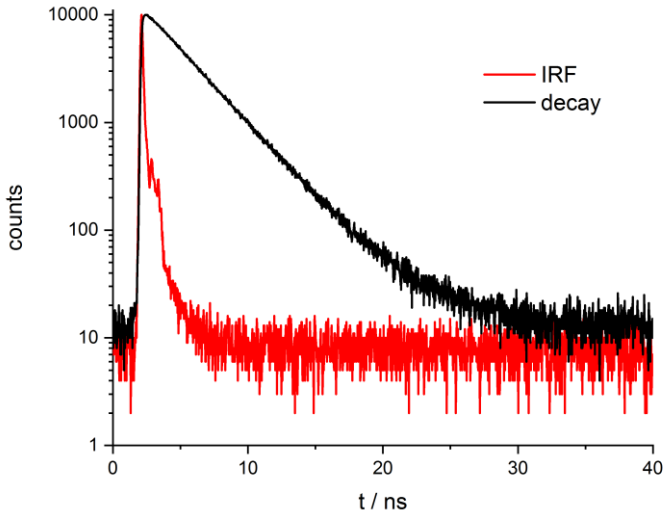

Figure S24. Fluorescence decay traces of **MesPtSPyr** in a 2-MeTHF matrix at 77 K. Decay can be fitted with a monoexponential decay with a lifetime of 3.19 ± 0.03 ns.

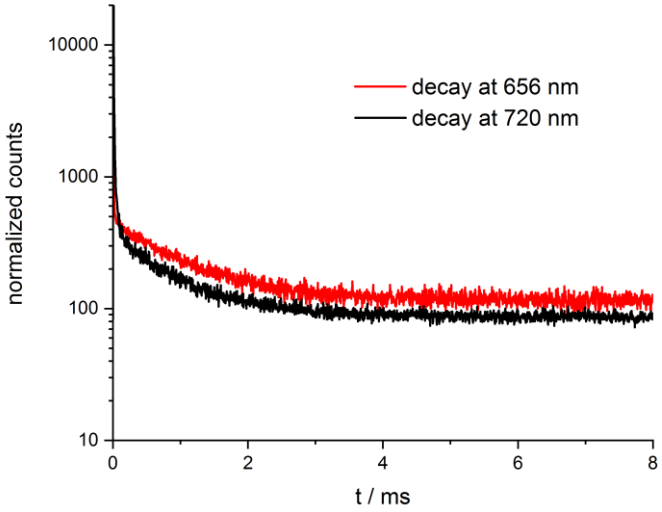

Figure S25. Phosphorescence decay traces of **MesPtSPyr** in a 2-MeTHF matrix at 77 K. Decay can be fitted with a monoexponential decay and a lifetime of 1.04 ± 0.06 ms.

UV/Vis and Quantum Chemical Calculations

Table S1. Absorption data for BPtSPyr and MesPtSPyr as well as TD-DFT-calculated band energies and assignments

absorption data		TD-DFT calculations[a]			
solvent	λ_{max}[b] (ε[c])	λ[b]	f[d]	m.c.[e]	assignment
		MesPtSPyr			
toluene	307 (14), 431 (25)	n.d.	n.d.	n.d.	n.d.
THF	306 (12), 431 (22)				
acetone	430 (23)				
		BPtSPyr			
toluene	418 (28), 469 (51), 499 (4)	392	0.37	H→L	ππ* BDP
THF	419 (29), 467 (51), 493 (4)	402	0.66	H→L+1	ππ* pyrS
acetone	416 (29), 465 (50), 483 (4)	567	0.05	H-1→L	PB-CT

[a]DFT calculations on the pbe1pbe/6-31G(d) level of therory; PCM model for CH_2Cl_2. [b]λ in nm. [c]ε / 10^3 M^{-1} cm^{-1}. [d]f = oscillator strength. [e]m.c. = major contribution. H refers to HOMO and L to LUMO.

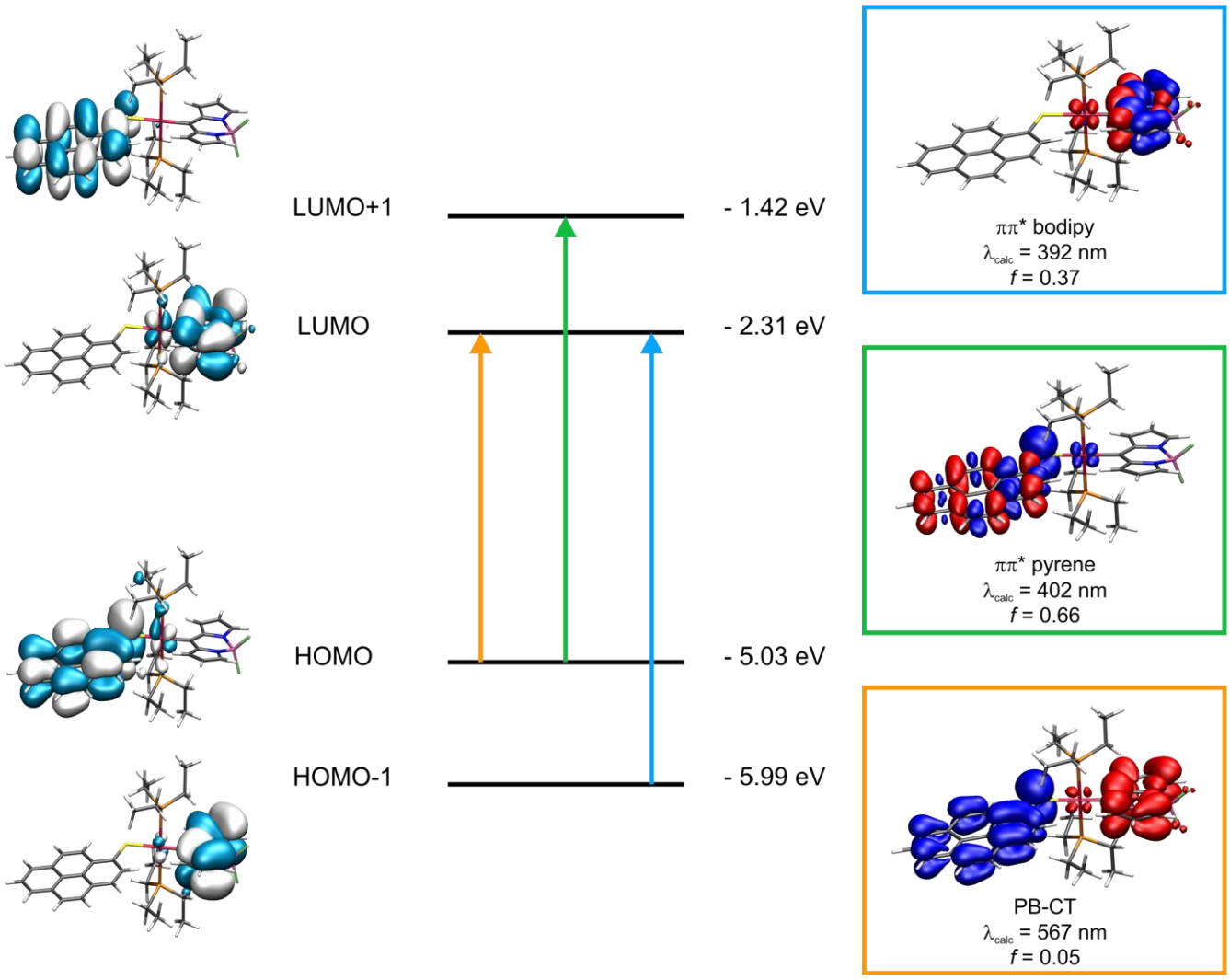

Figure S26. Graphical representation of the relevant MOs and TD-DFT energies of **BPtSPyr** in the neutral form as well as electron density difference maps (*blue* = electron density loss, *red* = electron density gain).

Table S2. Calculated Mulliken parameters of BPtSPyr in the neutral form. Fragment contributions are given in percent.

Orbital	Pt	PEt_3	bodipy	mercaptopyrene
LUMO+1	1	0	0	99
LUMO	4	2	94	0
HOMO	3	2	1	94
HOMO-1	1	1	98	0

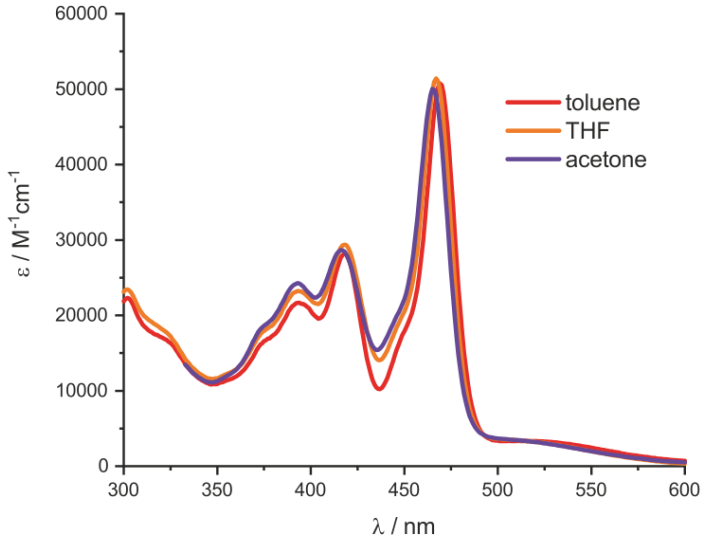

Figure S27. UV-Vis spectra of **BPtSPyr** in three different solvents.

Emission Spectroscopy of BPtSPyr

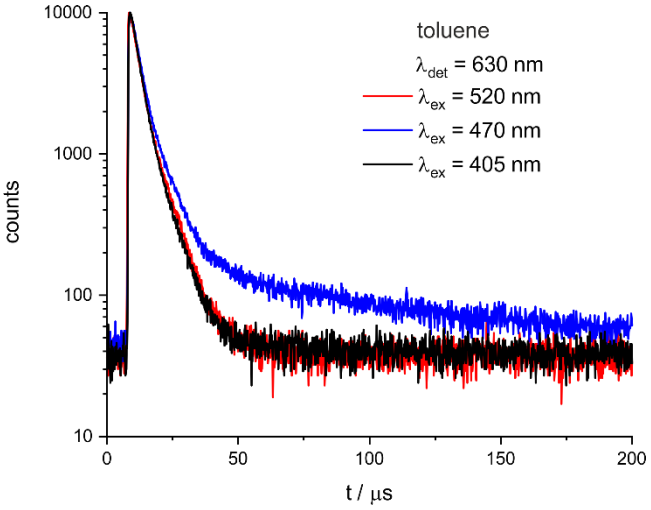

Figure S28. Emission decay traces of **BPtSPyr** detected at 630 nm in a deaerated and nitrogen-saturated 1 μM toluene solution at r.t. The blue curve has two components for the overlapping emission from the ^{3}BDP and the ^{3}PB-CT states.

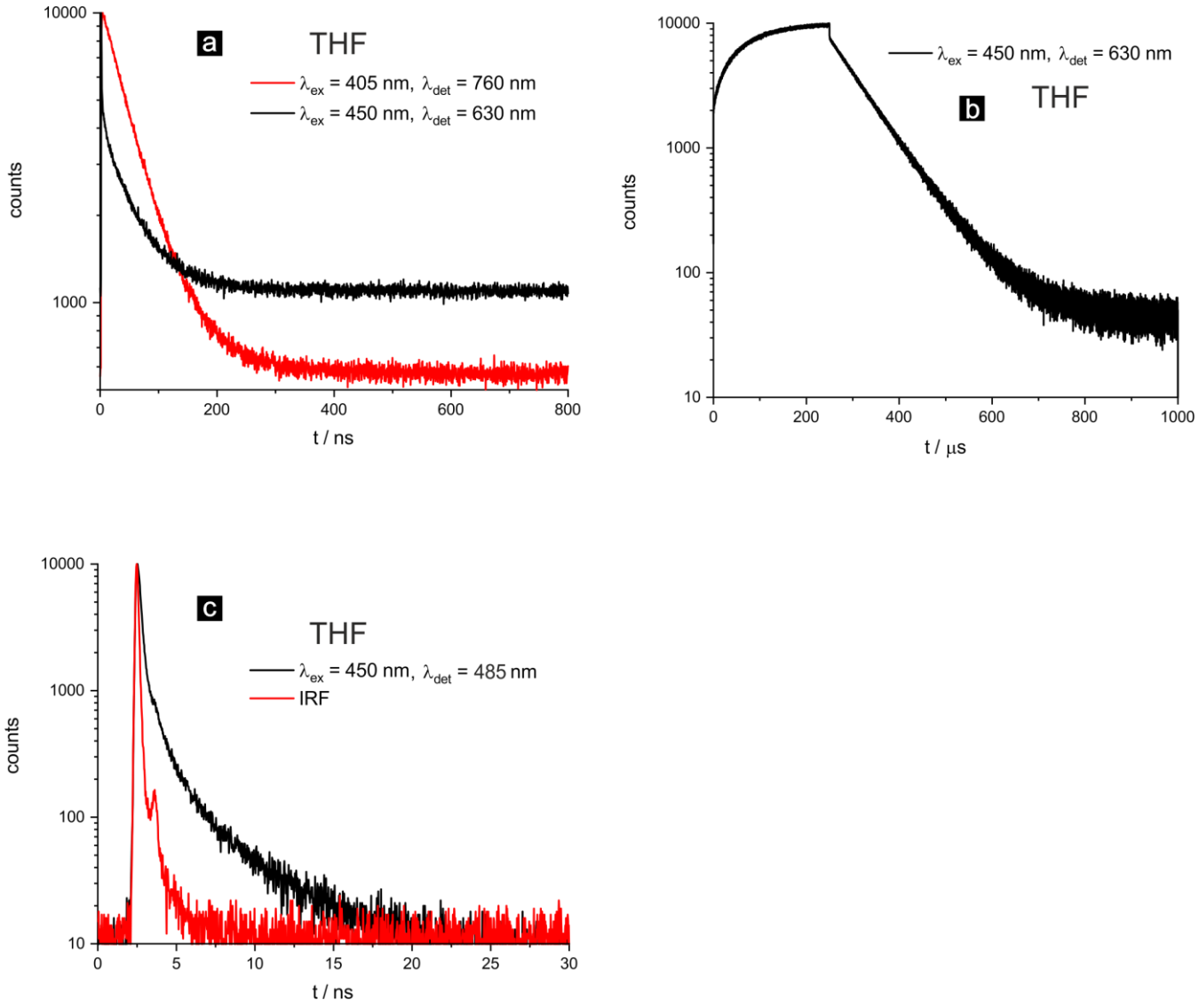

Figure S29. Emission decay traces of **BPtSPyr** in a deaerated and nitrogen-saturated 1 µM THF solution at r.t. In a) the 50 ns component is depicted; b) depicts the 78 µs component; c) shows the fluorescence lifetime decay. The rise time of 300 µs in Figure S29b is due to prior excited state saturation in the "burst mode".

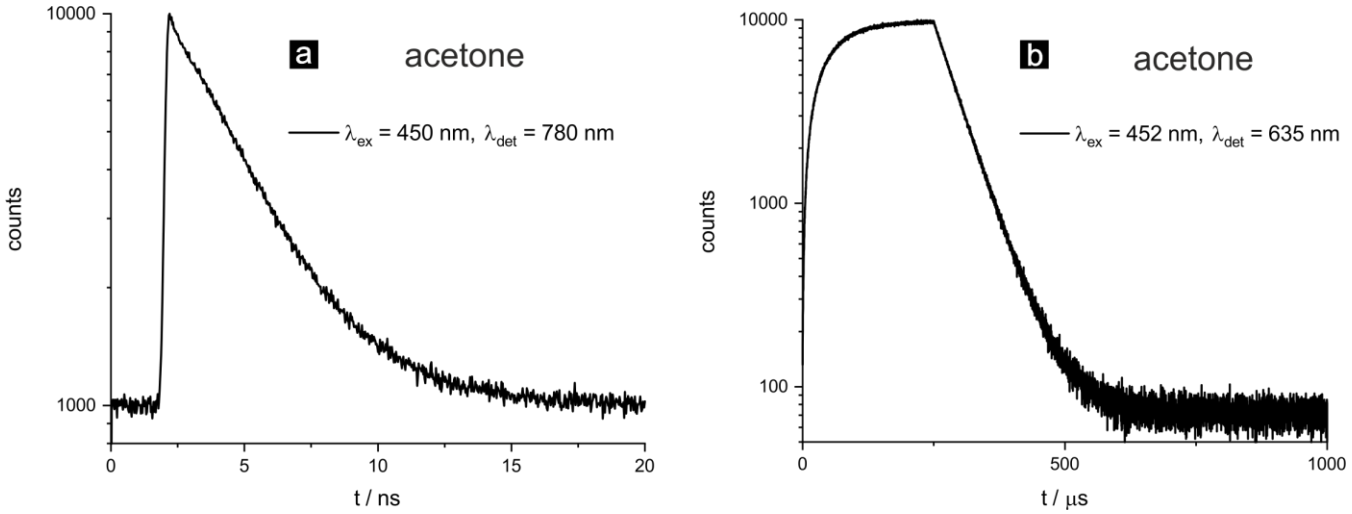

Figure S30. Emission decay traces of **BPtSPyr** in a deaerated and nitrogen-saturated 1 µM acetone solution at r.t. with a) depicting the 2.4 ns component and b) the 279 µs component. The rise time of 300 µs in Figure S30b is due to prior excited state saturation in the "burst mode".

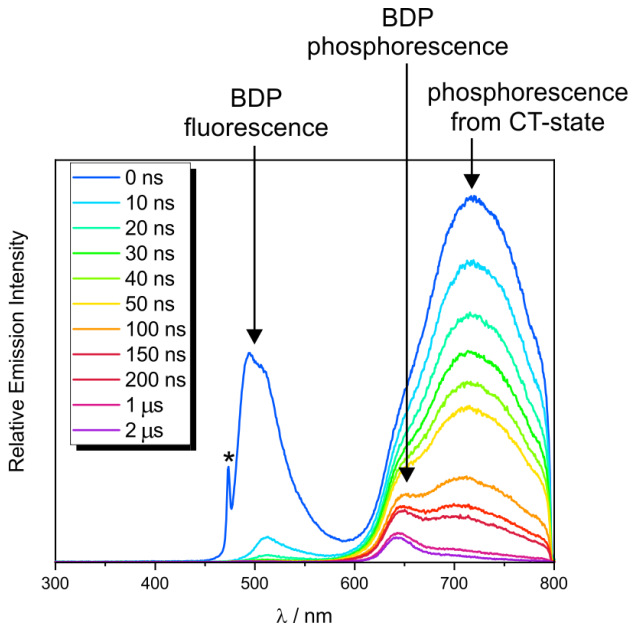

Figure S31. Transient emission spectra recorded after indicated delay times after laser excitation at 470 nm in a ca. 20 µM THF solution and time-integrated over 200 ns. *Residual excitation light. The shift of the NIR emission maximum in THF with respect to that in Figure 2 arises from its proximity to the low-energy limit of the detector.

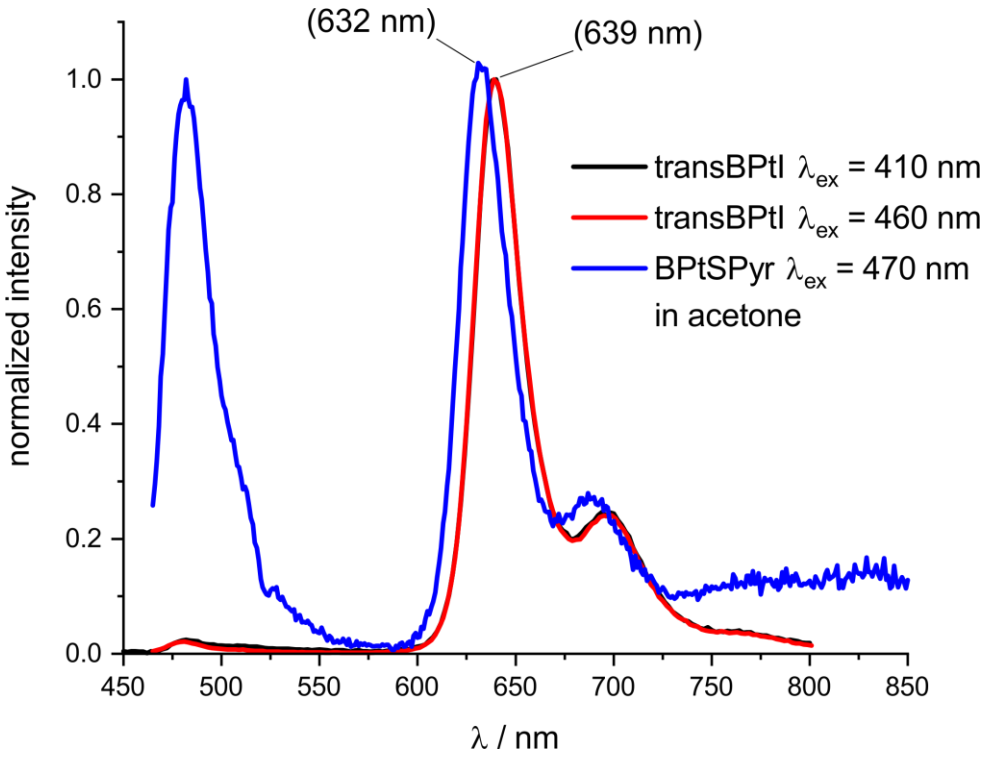

Figure S32. Comparison of the emission spectra of **BPtSPyr** (blue curve) and of **BPtI** at λ_{exc} = 410 nm (black curve) or λ_{exc} = 460 nm (red curve) in deaerated and nitrogen-saturated 1 μM acetone solutions at r.t. The different emission energies and intensity ratios of the fluorescence and phosphorescence emissions under identical conditions prove that the BDP-based emissions are also inherent features of **BPtSPyr** and are not due to contamination with the **BPtI** precursor.

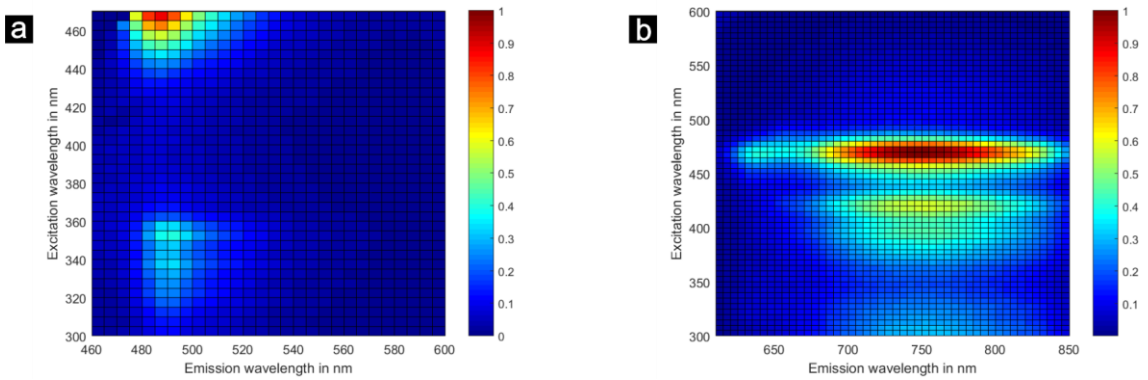

Figure S33. Emission vs. excitation maps recorded on a ca. 1 μM THF solution of **BPtSPyr** at r.t. for a) the fluorescence emission and b) the phosphorescence emission.

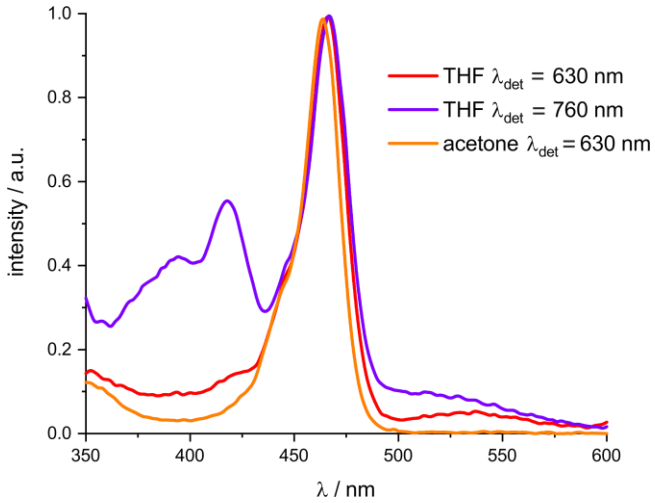

Figure S34. Excitation spectra of **BPtSPyr** recorded in ca. 1 μM THF or acetone solutions at r.t. with different detection wavelengths.

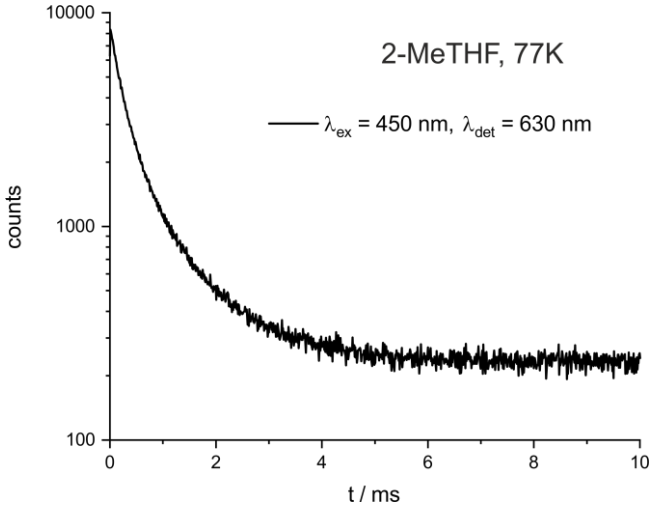

Figure S35. Emission decay trace of BPtSPyr in a 1 μM 2-MeTHF matrix at 77 K. The decay can be fitted with a biexponential model with decay times of 279 μs and 1.12 ms, which is due to the close energetic proximity of the two emissions.

Transient Absorption Spectroscopy

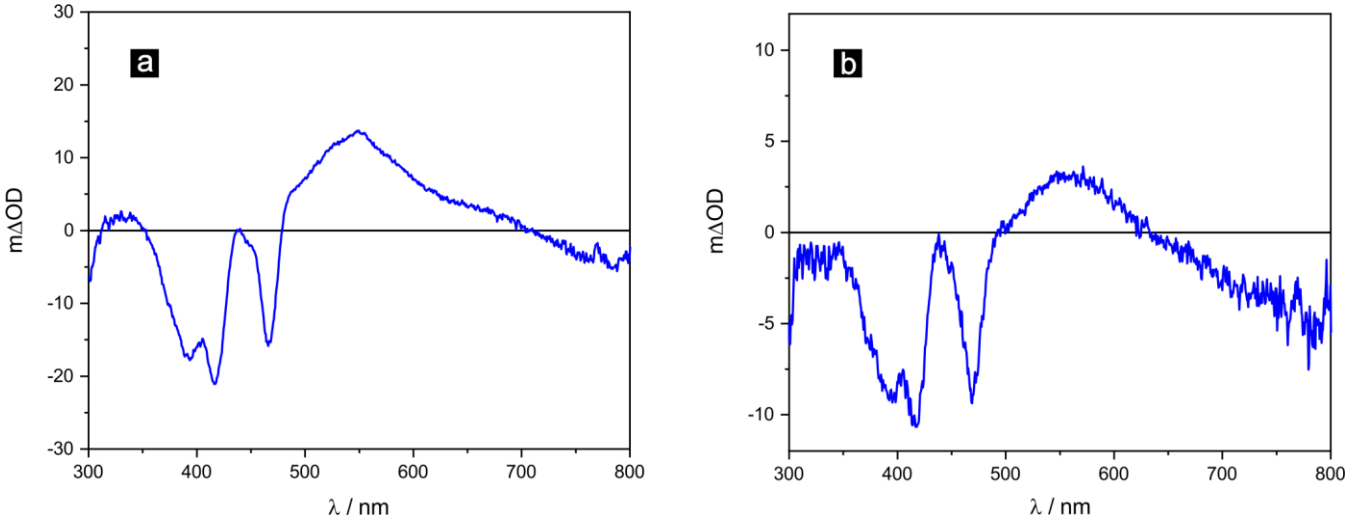

Figure S36. Transient absorption spectra of **BPtSPyr** recorded in a 20 μM THF solution at r.t. with laser excitation adjusted to a) 532 nm, or b) 410 nm time-integrated over 200 ns.

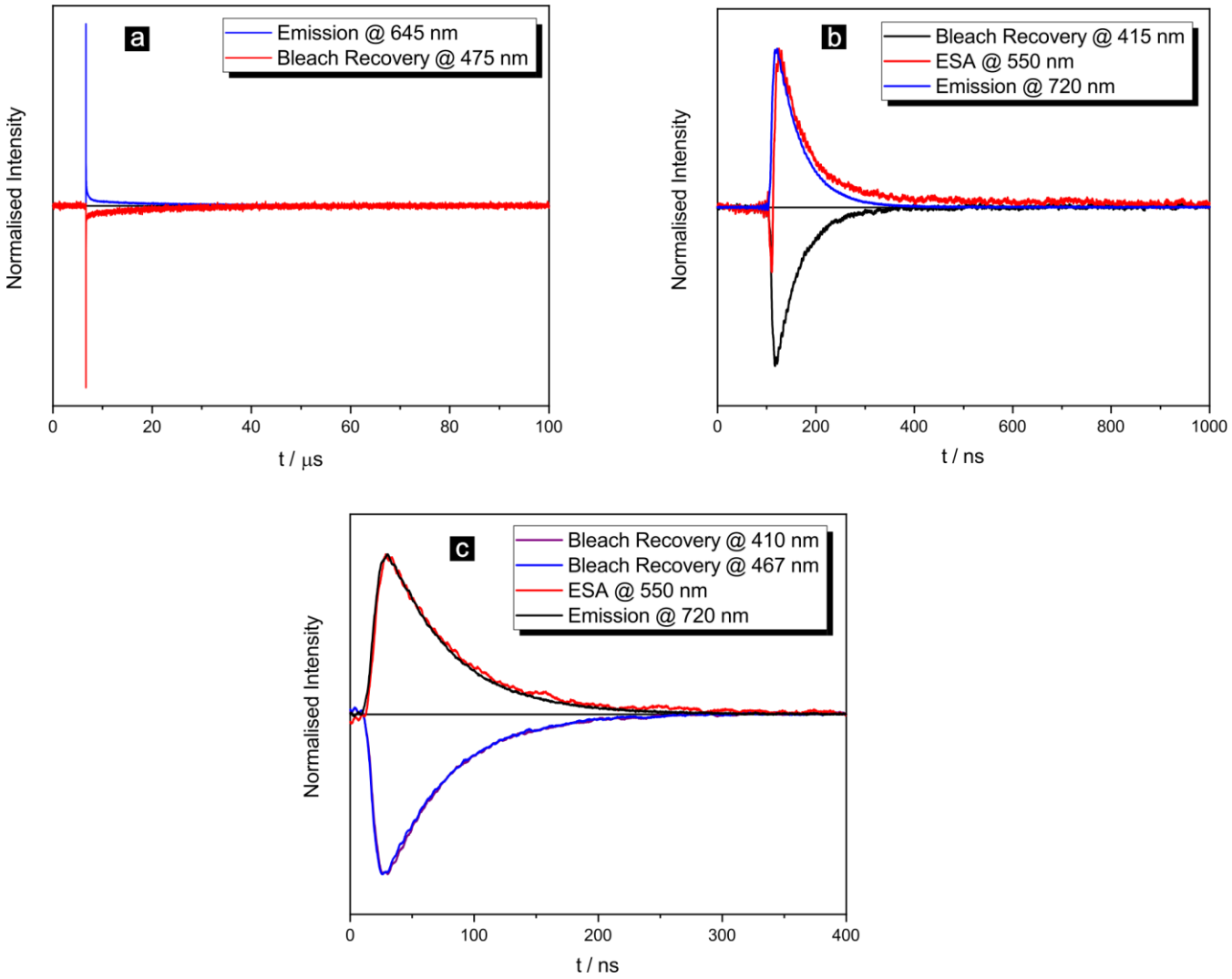

Figure S37. Single point kinetics of **BPtSPyr** recorded in 20 µM THF solution at r.t. after laser excitation at a,b) 470 nm, or c) 532 nm for the different features of the transient absorption spectrum. The exponential decays can be fitted with a lifetime of 16.5 µs for a) and 50 ns for b) and c).

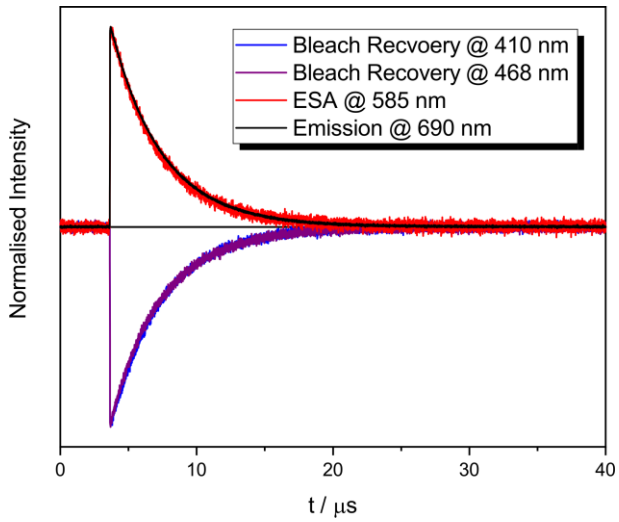

Figure S38. Single point kinetics of **BPtSPyr** recorded in 20 µM toluene solution at r.t. after laser excitation at 532 nm for the different features of the transient absorption spectm. The mono exponential decays can be fitted with a lifetime of 3.6 µs.

Electrochemistry

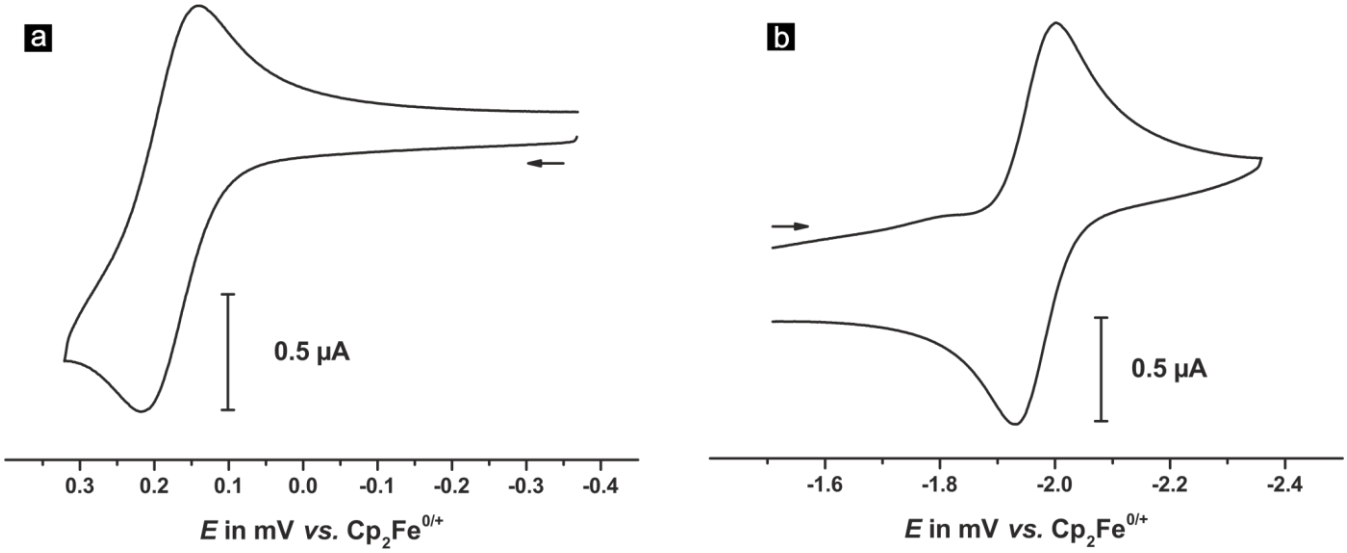

Figure S39. Cyclic voltammograms (ν = 100 mV/s) of a) the anodic and b) the cathodic sweep of **BPtSPyr** in THF at r.t. with NBu_4PF_6 (0.1 M) as the supporting electrolyte referenced to the $Cp_2Fe^{0/+}$ couple ($E_{1/2}$ =0.000 V).

Table S3. Electrochemical Data for BPtI and BPtSPyr[a]

complex	$E_{1/2}$ / mV (anodic sweep)	$E_{1/2}$ / mV (cathodic sweep)
BPtI		-1770
BPtSPyr	180	-1970

[a]All potentials are referenced to the $Cp_2Fe^{0/+}$ couple ($E_{1/2}$ =0.000 V) and were measured in CH_2Cl_2 at 293 K with NBu_4PF_6 as the supporting electrolyte.

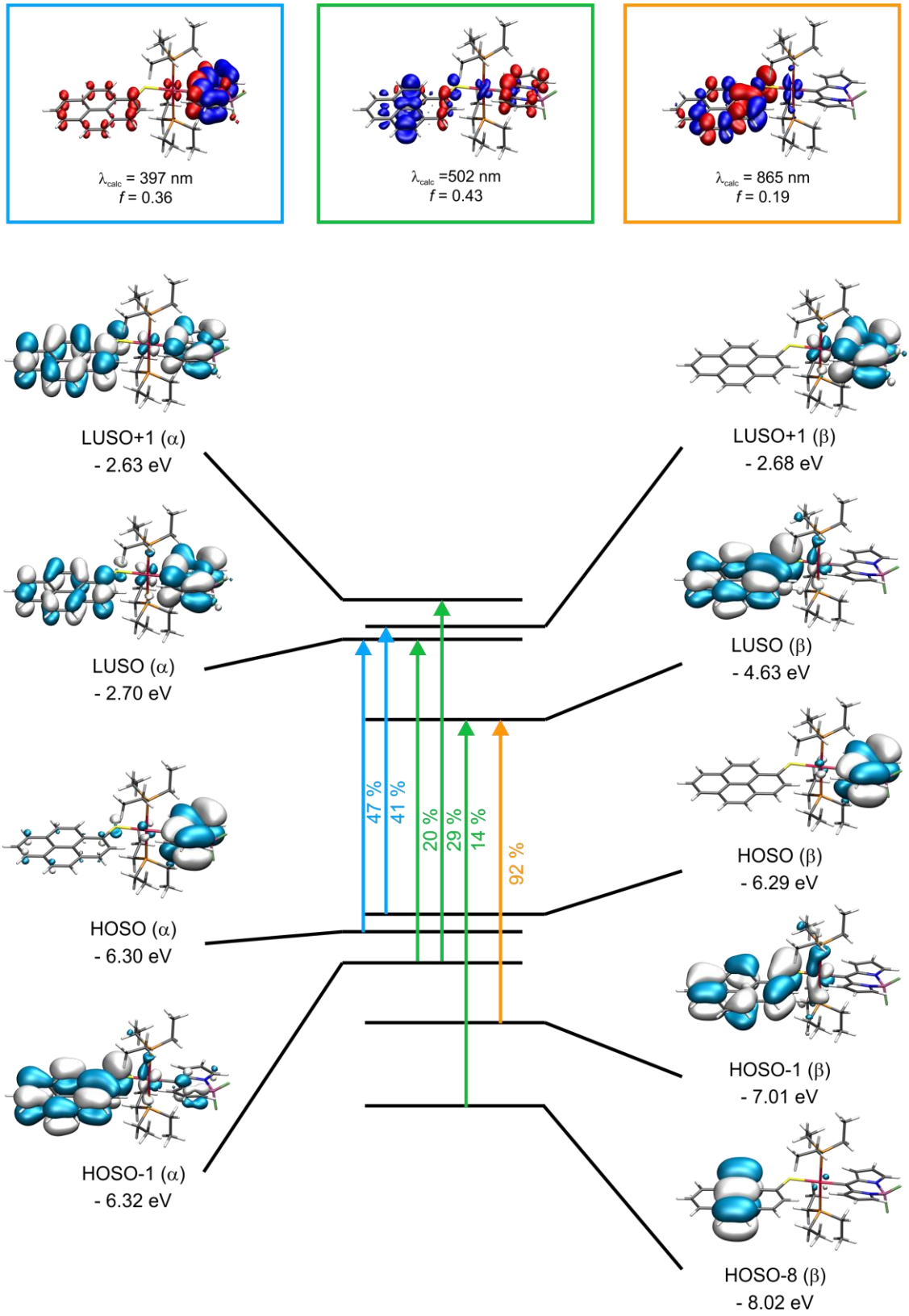

Figure S40. Graphical representations of the relevant spin orbitals and TD-DFT energies of **BPtSPyr** in the cationic form as well as electron density difference maps (*blue* = electron density loss, *red* = electron density gain).

Table S4. Calculated Mulliken parameters of BPtSPyr in the cationic form. Fragment contributions are given in percent.

Orbital	Pt	PEt_3	bodipy	mercaptopyrene
LUSO+1(β)	3	2	93	2
LUSO+1(α)	2	1	31	66
LUSO(β)	2	2	1	95
LUSO(α)	1	2	63	34
HOSO(α)	1	1	93	5
HOSO(β)	1	1	98	0
HOSO-1(α)	2	2	5	90
HOSO-1(β)	6	6	1	87
HOSO-8(β)	1	0	0	99

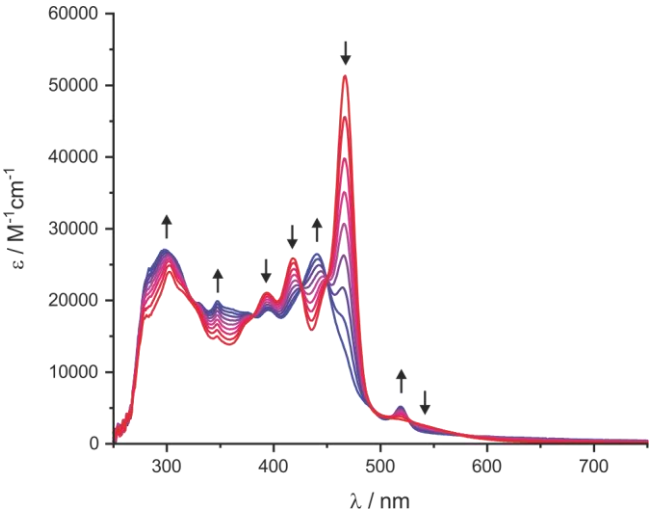

Figure S41. Changes of UV/Vis/NIR spectra of **BPtSPyr** on reductions (THF, NBu_4PF_6, 293 K).

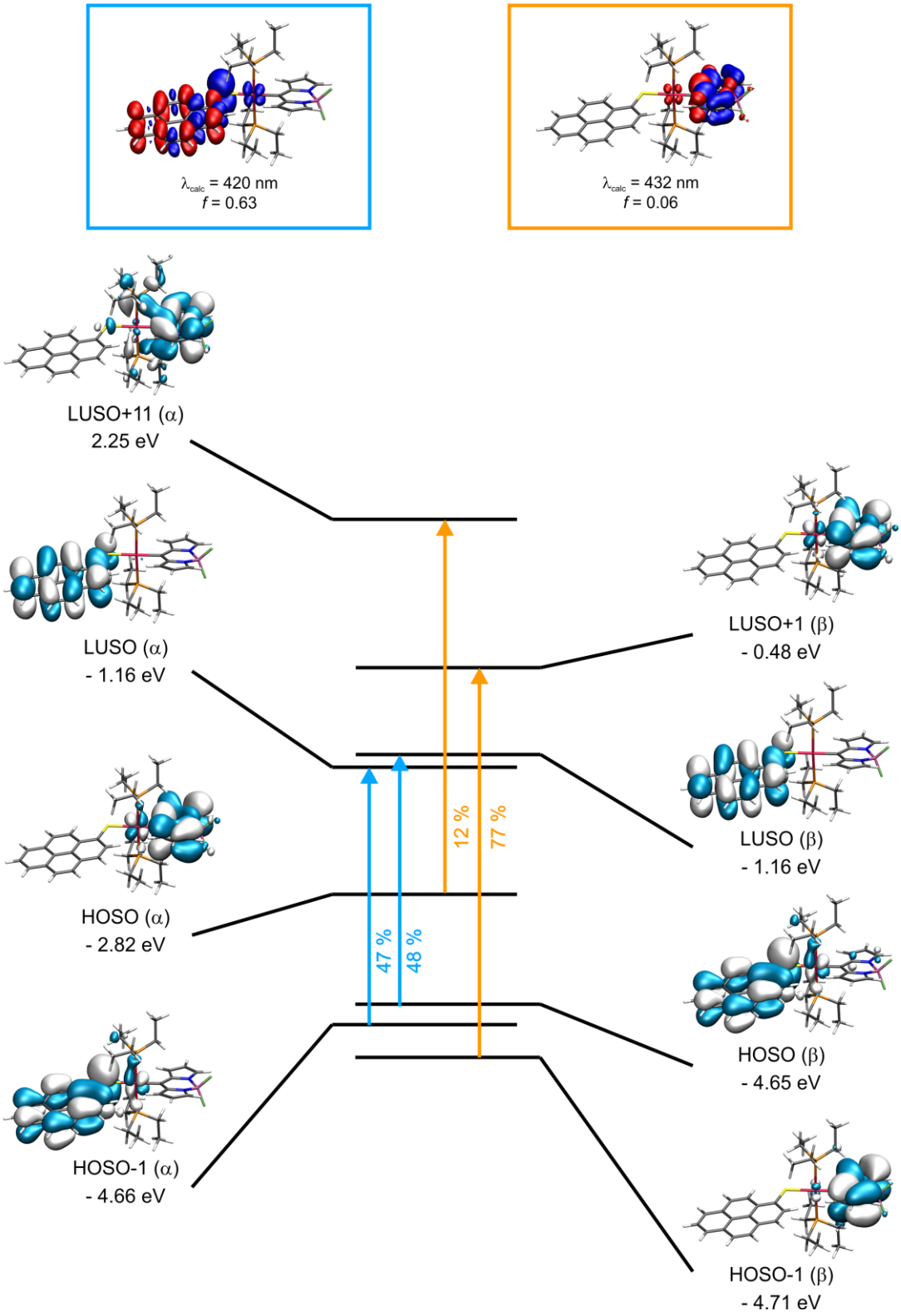

Figure S42. Graphical representations of the relevant spin orbitals and TD-DFT energies of **BPtSPyr** in the anionic form as well as electron density difference maps (*blue* = electron density loss, *red* = electron density gain).

Table S5. Calculated Mulliken parameters of BPtSPyr in the anionic form. Fragment contributions are given in percent.

Orbital	Pt	PEt_3	bodipy	mercaptopyrene
LUSO+11(α)	9	14	77	0
LUSO+1(β)	4	3	92	1
LUSO(β)	1	0	0	99
LUSO(α)	1	0	0	99
HOSO(α)	3	2	94	0
HOSO(β)	4	3	2	91
HOSO-1(α)	4	3	1	92
HOSO-1(β)	1	1	96	1

Table S6. Calculated spin density contributions of the respective fragments to the spin density surfaces of the radical cation and anion of BPtSPyr.

Oxidation State	cation	anion
Pt	-0.004	-0.002
PEt_3	0.023	0.017
bodipy	-0.004	0.990
mercaptopyrene	0.984	-0.006

Molecular Structures Obtained by Quantum Chemical Calculations

Table S7. Atomic coordinates of the optimized ground state geometry of BPtSPyr in the neutral form

Atom	x	y	z
Pt	0.85753	0.29072	-0.35315
B	5.49065	-1.06605	1.10122
F	5.73372	-2.41268	0.83786
F	6.59998	-0.48414	1.69619
N	5.12667	-0.33054	-0.21147
N	4.24586	-0.92401	2.01058
P	0.64512	-1.8441	-1.32242
P	1.10724	2.49799	0.43654
C	2.72634	-0.13259	0.25332
C	3.8367	0.0043	-0.6064
C	3.91647	0.52447	-1.91704
H	3.0707	0.88711	-2.48778
C	5.25475	0.50063	-2.2975
H	5.68257	0.83554	-3.2329
C	5.96476	-0.03869	-1.21555
H	7.02642	-0.22797	-1.12073
C	2.97273	-0.57741	1.57222
C	2.09945	-0.6984	2.67565
H	1.03894	-0.48145	2.65069
C	2.8552	-1.11431	3.76786
H	2.51279	-1.29731	4.77746
C	4.17318	-1.24381	3.31031
H	5.05809	-1.55068	3.85316
C	2.2037	-2.82444	-1.42058
H	2.91932	-2.21815	-1.98708
H	2.60775	-2.88129	-0.40283
C	2.08085	-4.21782	-2.03
H	3.06198	-4.70458	-2.03211
H	1.73071	-4.18363	-3.06668
H	1.39815	-4.85897	-1.46297
C	0.03115	-1.76713	-3.0547
H	-0.01609	-2.79357	-3.43789
H	-0.9961	-1.39247	-2.99162
C	0.86207	-0.87704	-3.97111
H	0.45322	-0.89522	-4.987
H	1.90625	-1.20351	-4.02761
H	0.84904	0.16073	-3.62076
C	-0.56388	-2.96631	-0.5074
H	-1.5025	-2.40646	-0.43722

H	-0.74263	-3.81278	-1.18226
C	-0.1275	-3.45479	0.86965
H	-0.93015	-4.0377	1.33335
H	0.11025	-2.61938	1.53608
H	0.75857	-4.09591	0.81308
C	2.86399	3.05635	0.53283
H	3.33791	2.43275	1.30069
H	3.34057	2.7755	-0.41209
C	3.09348	4.53634	0.82394
H	4.16878	4.73017	0.9007
H	2.63807	4.85459	1.76692
H	2.70161	5.17542	0.02622
C	0.47862	2.81214	2.14154
H	0.9235	2.04019	2.78087
H	0.89536	3.77173	2.4699
C	-1.03926	2.82706	2.28272
H	-1.31141	2.96299	3.33501
H	-1.49128	1.8942	1.93462
H	-1.48741	3.65041	1.71747
C	0.27747	3.7567	-0.61301
H	-0.78814	3.50686	-0.61358
H	0.39201	4.73408	-0.12836
C	0.80779	3.78039	-2.04259
H	0.6677	2.80706	-2.52599
H	1.87449	4.02708	-2.08195
H	0.27072	4.52968	-2.63357
S	-1.3789	0.80589	-1.14951
C	-2.58324	0.14241	-0.05091
C	-3.96532	0.22373	-0.37986
C	-2.2237	-0.45556	1.16858
C	-4.93729	-0.28863	0.53007
C	-4.43124	0.80883	-1.60268
C	-3.16909	-0.96172	2.0471
H	-1.16697	-0.519	1.41726
C	-6.32756	-0.20365	0.21758
C	-4.53682	-0.88957	1.7583
C	-5.75565	0.88943	-1.90146
H	-3.69558	1.19395	-2.30179
H	-2.84538	-1.41862	2.97997
C	-6.75324	0.39045	-1.00468
C	-7.3009	-0.71237	1.1282
C	-5.53443	-1.39388	2.65212
H	-6.07933	1.33887	-2.83745
C	-8.12358	0.46687	-1.2926
C	-8.65993	-0.61414	0.79935

C	-6.85825	-1.30999	2.35413
H	-5.20713	-1.84886	3.58434
C	-9.06402	-0.0306	-0.39761
H	-8.44306	0.9217	-2.22721
H	-9.40035	-1.00201	1.49498
H	-7.60661	-1.69579	3.04215
H	-10.1226	0.03619	-0.63421

Table S8. Atomic coordinates of the optimized ground state geometry of BPtSPyr in the cationic form

Pt	0.83696	0.27223	-0.31157
B	5.51449	-0.98943	0.9736
F	5.6453	-2.34494	0.67998
F	6.68656	-0.48383	1.50539
N	5.11361	-0.21852	-0.31014
N	4.33164	-0.7855	1.95413
P	0.73877	-1.90917	-1.23363
P	1.05924	2.50569	0.44941
C	2.73826	-0.06591	0.2449
C	3.80463	0.09039	-0.66048
C	3.82742	0.60914	-1.97577
H	2.95776	0.95785	-2.51915
C	5.15065	0.61074	-2.4008
H	5.5398	0.95489	-3.34942
C	5.90897	0.08491	-1.34291
H	6.97614	-0.08761	-1.28691
C	3.03581	-0.47061	1.56236
C	2.21304	-0.56099	2.70868
H	1.15034	-0.3534	2.72734
C	3.02323	-0.92482	3.77825
H	2.73088	-1.07054	4.80925
C	4.32195	-1.05836	3.26487
H	5.23374	-1.33855	3.77654
C	2.3577	-2.76633	-1.4214
H	2.97961	-2.12583	-2.05599
H	2.84213	-2.76624	-0.4382
C	2.29072	-4.18142	-1.98917
H	3.30465	-4.58781	-2.06342
H	1.85542	-4.20387	-2.9932
H	1.71284	-4.85765	-1.35132
C	0.00305	-1.90002	-2.92083
H	0.01511	-2.93235	-3.28995
H	-1.0502	-1.62081	-2.80127
C	0.6956	-0.96218	-3.90317
H	0.21393	-1.02593	-4.88424
H	1.7525	-1.21608	-4.03562

H	0.63642	0.07883	-3.56669
C	-0.32896	-3.09993	-0.32421
H	-1.32136	-2.64228	-0.24657
H	-0.44267	-3.98724	-0.95921
C	0.19895	-3.48517	1.05333
H	-0.51302	-4.14787	1.55551
H	0.35171	-2.60695	1.68875
H	1.15549	-4.01364	0.98789
C	2.79708	3.11759	0.46502
H	3.33185	2.4999	1.19612
H	3.23138	2.87121	-0.50927
C	2.98591	4.6001	0.7741
H	4.05572	4.83347	0.77331
H	2.5938	4.87596	1.75754
H	2.51126	5.24124	0.02471
C	0.47302	2.83634	2.16289
H	1.07351	2.20156	2.8251
H	0.74043	3.87498	2.39094
C	-1.01548	2.61619	2.40175
H	-1.26139	2.85839	3.44082
H	-1.30647	1.57739	2.22422
H	-1.63078	3.25534	1.76031
C	0.1492	3.70735	-0.60387
H	-0.91301	3.44469	-0.55493
H	0.25462	4.69872	-0.14689
C	0.62725	3.71611	-2.05227
H	0.52509	2.7263	-2.51145
H	1.67739	4.01609	-2.13302
H	0.03315	4.42245	-2.64077
S	-1.39703	0.70367	-1.07735
C	-2.5965	0.05314	-0.0481
C	-3.99171	0.1981	-0.3932
C	-2.25641	-0.61983	1.15559
C	-4.97615	-0.33007	0.48953
C	-4.42356	0.8457	-1.57929
C	-3.21583	-1.12508	1.99253
H	-1.20368	-0.72565	1.40176
C	-6.35559	-0.19804	0.17754
C	-4.59575	-0.99491	1.69041
C	-5.75528	0.97205	-1.87941
H	-3.68291	1.2479	-2.26219
H	-2.92334	-1.63389	2.90716
C	-6.7586	0.4582	-1.01538
C	-7.34233	-0.7229	1.05893
C	-5.59243	-1.51073	2.5527

H	-6.05792	1.47352	-2.79452
C	-8.13224	0.57948	-1.30685
C	-8.70247	-0.579	0.72918
C	-6.92459	-1.37952	2.24952
H	-5.28561	-2.01552	3.46424
C	-9.08991	0.06588	-0.4419
H	-8.43475	1.08248	-2.22135
H	-9.45336	-0.9806	1.40427
H	-7.67999	-1.77931	2.92026
H	-10.14415	0.16695	-0.67953

Table S9. Atomic coordinates of the optimized ground state geometry of BPtSPyr in the anionic form

Pt	0.83493	0.29354	-0.38434
B	5.4689	-1.01715	1.13749
F	5.76969	-2.38336	0.93466
F	6.59285	-0.4184	1.73252
N	5.1307	-0.33815	-0.1926
N	4.2349	-0.86746	2.03286
P	0.67126	-1.84617	-1.31051
P	1.15253	2.46551	0.4174
C	2.72479	-0.13498	0.24066
C	3.85025	-0.01057	-0.61961
C	3.95692	0.45797	-1.9435
H	3.12341	0.80333	-2.54351
C	5.32207	0.40649	-2.30463
H	5.76096	0.70412	-3.24981
C	6.00856	-0.08766	-1.20871
H	7.06605	-0.27875	-1.0782
C	2.96121	-0.53718	1.58665
C	2.09075	-0.64881	2.68912
H	1.02668	-0.44559	2.65855
C	2.86175	-1.0493	3.80325
H	2.51145	-1.21956	4.81452
C	4.16786	-1.17421	3.36218
H	5.06012	-1.46283	3.90298
C	2.23961	-2.80871	-1.4053
H	2.95358	-2.17919	-1.94835
H	2.62994	-2.86347	-0.38262
C	2.14184	-4.19632	-2.03105
H	3.124	-4.68151	-2.01068
H	1.82055	-4.15451	-3.07748
H	1.44482	-4.84674	-1.49132
C	0.02783	-1.83323	-3.03705
H	-0.01248	-2.86949	-3.39421
H	-1.00334	-1.46935	-2.96749

C	0.83136	-0.95588	-3.98924
H	0.40633	-0.99744	-4.99842
H	1.87818	-1.27245	-4.05311
H	0.8173	0.08721	-3.65542
C	-0.51551	-2.98164	-0.47185
H	-1.45975	-2.43115	-0.39635
H	-0.69413	-3.8417	-1.12992
C	-0.05674	-3.44322	0.90747
H	-0.85469	-4.00509	1.40545
H	0.21488	-2.59559	1.54599
H	0.81973	-4.09721	0.84331
C	2.91642	2.99996	0.5131
H	3.37247	2.37315	1.28803
H	3.39174	2.68974	-0.42367
C	3.16924	4.47892	0.78857
H	4.24696	4.65794	0.87296
H	2.71077	4.81686	1.72396
H	2.79443	5.11706	-0.01881
C	0.5423	2.79897	2.12762
H	1.00642	2.03556	2.76359
H	0.94895	3.7683	2.44104
C	-0.97336	2.79115	2.28828
H	-1.23958	2.93022	3.34222
H	-1.41124	1.84743	1.95055
H	-1.44362	3.60069	1.72021
C	0.33702	3.76051	-0.60657
H	-0.73188	3.52226	-0.60961
H	0.46329	4.73099	-0.11021
C	0.86154	3.79927	-2.03807
H	0.70799	2.83357	-2.53262
H	1.9324	4.02821	-2.0763
H	0.33533	4.56443	-2.61945
S	-1.42784	0.8212	-1.17968
C	-2.62754	0.15398	-0.08713
C	-4.0171	0.24004	-0.39149
C	-2.25401	-0.46264	1.12195
C	-4.97732	-0.28226	0.52529
C	-4.50024	0.83999	-1.59934
C	-3.18759	-0.97615	2.00713
H	-1.19255	-0.53235	1.35
C	-6.37223	-0.19246	0.23363
C	-4.56069	-0.89863	1.74037
C	-5.82877	0.92608	-1.87976
H	-3.77098	1.23161	-2.30171
H	-2.85149	-1.4455	2.92972

C	-6.81464	0.41699	-0.97564
C	-7.33374	-0.71194	1.15177
C	-5.54562	-1.41236	2.64118
H	-6.16498	1.38727	-2.80577
C	-8.18917	0.49747	-1.24341
C	-8.69748	-0.60891	0.84258
C	-6.87439	-1.32454	2.36378
H	-5.20519	-1.87908	3.56311
C	-9.11741	-0.01058	-0.3415
H	-8.52112	0.96381	-2.16809
H	-9.42851	-1.00495	1.54373
H	-7.61315	-1.71839	3.0578
H	-10.17929	0.05962	-0.56272

References

(1) Irmler, P.; Winter, R. F. *Dalton Trans.* **2016**, *45*, 10420.
(2) Krejčik, M.; Daněk, M.; Hartl, F. *J. Electroanal. Chem. Interfacial Electrochem.* **1991**, *317*, 179.
(3) Frisch, M. J.; Trucks, G. W.; Schlegel, H. B.; Scuseria, G. E.; Robb, M. A.; Cheeseman, J. R.; Scalmani, G.; Barone, V.; Mennucci, B.; Petersson, G. A.; Nakatsuji, H.; Caricato, M.; Li, X.; Hratchian, H. P.; Izmaylov, A. F.; Bloino, J.; Zheng, G.; Sonnenberg, J. L.; Hada, M.; Ehara, M.; Toyota, K.; Fukuda, R.; Hasegawa, J.; Ishida, M.; Nakajima, T.; Honda, Y.; Kitao, O.; Nakai, H.; Vreven, T.; Montgomery Jr., J. A.; Peralta, J. E.; Ogliaro, F.; Bearpark, M. J.; Heyd, J.; Brothers, E. N.; Kudin, K. N.; Staroverov, V. N.; Kobayashi, R.; Normand, J.; Raghavachari, K.; Rendell, A. P.; Burant, J. C.; Iyengar, S. S.; Tomasi, J.; Cossi, M.; Rega, N.; Millam, N. J.; Klene, M.; Knox, J. E.; Cross, J. B.; Bakken, V.; Adamo, C.; Jaramillo, J.; Gomperts, R.; Stratmann, R. E.; Yazyev, O.; Austin, A. J.; Cammi, R.; Pomelli, C.; Ochterski, J. W.; Martin, R. L.; Morokuma, K.; Zakrzewski, V. G.; Voth, G. A.; Salvador, P.; Dannenberg, J. J.; Dapprich, S.; Daniels, A. D.; Farkas, O. d. o. n.; Foresman, J. B.; Ortiz, J. V.; Cioslowski, J.; Fox, D. J.; Gaussian, Inc.: Wallingford, CT, USA, 2009.
(4) Gunnarsson, O.; Lundqvist, B. I. *Phys. Rev. B* **1976**, *13*, 4274.
(5) Küchle, W.; Dolg, M.; Stoll, H.; Preuss, H. *J. Chem. Phys.* **1994**, *100*, 7535.
(6) Dolg, M.; Stoll, H.; Preuss, H. *J. Chem. Phys.* **1989**, *90*, 1730.
(7) Andrae, D.; Häußermann, U.; Dolg, M.; Stoll, H.; Preuß, H. *Theor. Chim. Acta* **1990**, *77*, 123.
(8) Hariharan, P. C.; Pople, J. A. *Theor. Chim. Acta* **1973**, *28*, 213.
(9) Perdew, J. P.; Burke, K.; Ernzerhof, M. *Phys. Rev. Lett.* **1996**, *77*, 3865.
(10) Adamo, C.; Barone, V. *J. Chem. Phys.* **1999**, *110*, 6158.
(11) Cancés, E.; Mennucci, B.; Tomasi, J. *J. Chem. Phys.* **1997**, *107*, 3032.
(12) Mennucci, B.; Tomasi, J. *J. Chem. Phys.* **1997**, *106*, 5151.
(13) Cossi, M.; Rega, N.; Scalmani, G.; Barone, V. *J. Comput. Chem.* **2003**, *24*, 669.
(14) Scalmani, G.; Frisch, M. J. *J. Chem. Phys.* **2010**, *132*, 114110.
(15) Runge, E.; Gross, E. K. U. *Phys. Rev. Lett.* **1984**, 52, 997.
(16) O'Boyle, N. M.; Tenderholt, A. L.; Langner, K. M. *J. Comput. Chem.* **2008**, *29*, 839.